



ELSEVIER

Contents lists available at ScienceDirect

## Quaternary Science Reviews

journal homepage: [www.elsevier.com/locate/quascirev](http://www.elsevier.com/locate/quascirev)



# Pre-glacial and post-glacial history of the Scandinavian Ice Sheet in NW Russia – Evidence from Lake Ladoga

E. Lebas <sup>a,\*</sup>, R. Gromig <sup>b</sup>, S. Krastel <sup>a</sup>, B. Wagner <sup>b</sup>, G. Fedorov <sup>c,d</sup>, C. Görtz <sup>a</sup>, T. Averes <sup>a</sup>, D. Subetto <sup>e,f,g</sup>, M. Naumenko <sup>h</sup>, M. Melles <sup>b</sup>

<sup>a</sup> Institute of Geosciences, University of Kiel, Kiel, Germany

<sup>b</sup> Institute of Geology and Mineralogy, University of Cologne, Cologne, Germany

<sup>c</sup> St. Petersburg State University, Institute of Earth Sciences, Russian Federation

<sup>d</sup> Arctic and Antarctic Research Institute, St. Petersburg, Russia

<sup>e</sup> Herzen State Pedagogical University of Russia, Saint-Petersburg, Russian Federation

<sup>f</sup> Northern Water Problems Institute of Karelian Research Centre, Russian Academy of Sciences, Petrozavodsk, Russian Federation

<sup>g</sup> Institute for Water and Environmental Problems, Siberian Branch of the Russian Academy of Sciences, Barnaul, Russian Federation

<sup>h</sup> St. Petersburg Federal Research Center of the Russian Academy of Sciences, Institute of Limnology, 9, Sevastyanova St., St. Petersburg, 196105, Russian Federation



## ARTICLE INFO

### Article history:

Received 30 April 2020

Received in revised form

10 September 2020

Accepted 30 September 2020

Available online xxx

### Keywords:

Seismic stratigraphy

Seismic geomorphology

Moraine-mound complex

Moraine

Early Weichselian

Valdai glaciation

Saalian

Moscow glaciation

Quaternary

## ABSTRACT

Lacustrine sedimentary records are valuable archives of regional paleoenvironmental and paleoclimatic changes. High-resolution seismic reflection data collected in 2013, in conjunction with data from sediment core Co1309, provide a detailed reconstruction of the preglacial and postglacial environmental and sedimentological history of Lake Ladoga (NW Russia) during the late Quaternary. The exceptionally good quality of the seismic data reveals an up to 90-m-thick sedimentary infill in undisturbed places, containing four distinct sequences documented in unprecedented detail. The deepest sequence S1 most likely represents the bedrock of the lacustrine basin, which was reshaped during the subsequent glaciations. The overlying sequence S2 contains large-scale mounds of variable dimension, shape and internal architecture, which suggest a complex history of formation and deformation. We interpret these mounds as a moraine-mound complex resulting from thrusting and bulldozing processes of pre-existing, subglacial sediments during the overall retreat of the Scandinavian Ice Sheet following the Last Glacial Maximum. The finely-layered sequence S3 coincides with varved sediments in core Co1309 that mark the Scandinavian Ice Sheet deglaciation in the Ladoga basin. The youngest sequence S4, characterised by a semi-transparent facies in the acoustic data, coincides with lacustrine sediments in core Co1309 that were deposited during the Holocene. Our results also document major thoroughgoing fault systems in the northwestern part of the lake basin, along with unconformities related to lake-level fluctuations, notably in the eastern-, western- and southernmost regions. By coupling hydroacoustic and sedimentological data, we are able to pinpoint lateral variations and modifications of sedimentary inputs through time during the evolution of the Ladoga basin, along with unravelling the paleoenvironmental history of Lake Ladoga since the pre-LGM.

© 2020 Elsevier Ltd. All rights reserved.

## 1. Introduction

Lacustrine sedimentary records are valuable archives of regional environmental and climatic changes, past tectonic and volcanic

events, bottom water dynamics, and of the origin and development of lake basins. They can provide a continuous and high-resolution record of changing conditions and processes that occur in a lake and in the catchment area, which allows for a better reconstruction of the paleoclimatic and paeoenvironmental conditions of an area, over long time scales (e.g. Beres et al., 2008; Melles et al., 2012; Johnson et al., 2016; Hang et al., 2019). Recent advances in geophysical techniques allowed improvement of our understanding on the formation and evolution of lacustrine basins

\* Corresponding author. Université de Paris, Institut de physique du globe de Paris, CNRS, F-75005, Paris, France.

E-mail address: [elebas@ipgp.fr](mailto:elebas@ipgp.fr) (E. Lebas).

considerably. In formerly glaciated regions, lacustrine infills may contain critical information on deglaciation processes and past ice-sheet dynamics, which might be missing on land (e.g. Charlet et al., 2008; Waldmann et al., 2010; Greenwood et al., 2015; Lebas et al., 2019). It is, hence, crucial, to acquire acoustic imagery and profiling in such basins as buried glacial landforms represent key geomorphological indicators to constrain the growth, past dynamics and decay of former ice masses (Amantov and Amantova, 2014). Improvement in depth penetration and resolution of these acoustic techniques unravelled previously unreported glacial landforms that allowed for a more detailed reconstruction of the location and dynamics of former ice sheets (e.g. Dowdeswell et al., 2010; Batchelor et al., 2016, 2017). Such observations are critical as they provide constraints for numerical models assessing ice-sheet responses to past climate changes by allowing to infer the conditions that persisted in these environments during the past glaciations. Integration of geophysical data, in conjunction with sedimentological data provide all the necessary information to reconstruct a most complete and detailed preglacial and postglacial history of lacustrine basins.

Lake Ladoga, situated in NW Russia (Fig. 1), has been investigated in many studies (e.g. Kvasov, 1979; Davydova, 1990; Bakhmutov et al., 1993; Mandysh and Shilkrot, 1995; Saarnisto and Grönlund, 1996; Davydova et al., 1998; Subetto et al., 1998; Aleksandrovskii et al., 2009; Subetto, 2009; Saarnisto, 2012; and reference therein), but the Weichselian (MIS5d-MIS2; known in Russia as Valdai) history remained insufficiently known and is mostly reconstructed based on terrestrial sediments (Miettinen et al., 2005) and on-land geomorphological evidence (e.g. Kalm, 2012; Hughes et al., 2016). This fragmentary history is partly due to the widespread erosion of the Scandinavian Ice Sheet (SIS) that inundated the region during the Last Glacial Maximum (LGM), along with a lack of dated records. The post-LGM history has been relatively well studied over the last decades, but little is still known about the pre-LGM history of Lake Ladoga. A drilling campaign carried out in 1934, in the southwestern part of the lake basin (Fig. 1a and b), recovered some ~40-m-long sediment cores that provided rudimentary lithological information on the drilled sediments. According to the original investigations, the sediments consisted of marine interglacial clays, glacial till and glacio-limnic varved clays interbedded with postglacial sand (Krasnov and Reineke, 1936). Unfortunately, these records do not exist anymore. Some additional insights into the preglacial history of Lake Ladoga are provided by initial hydroacoustic surveys, which, however, were carried out with a sparse coverage of the data sets (Amantov, 2014; Amantov and Amantova, 2014).

In the framework of the Russian-German project PLOT (Paleolimnological Transect) extensive fieldwork (including seismic surveys, coring, and hydrological investigations) was conducted between 2013 and 2017 on a number of northern Eurasian lakes to investigate the late Quaternary climatic and environmental history across the Russian Arctic (e.g. Melles et al., 2019). At Lake Ladoga, ~1500 km of multi-channel seismic (MCS) reflection profiles were acquired, covering most of the lacustrine basin (this paper). A 22.75-m-long sediment core (Co1309) was also retrieved in the northwestern lake basin, which provided new constraints on the preglacial (e.g. Andreev et al., 2019; Gromig et al., 2019) and postglacial (e.g. Savelieva et al., 2019; Kostrova et al., 2019) history of the lake.

The study presented here aims at reconstructing the depositional environments of Lake Ladoga during its preglacial and postglacial history using the large, new set of MCS data gathered during the PLOT project, along with recently-published sediment core data. The limited penetration depth and small coverage of past acoustic and coring data available on Lake Ladoga left several

unanswered questions regarding the deepest sedimentary sequences. Hence, the present paper aims at (i) better understanding the origin and evolution of the entire lake infill, including past lake-level fluctuations and tectonic activity, (ii) assessing in detail the pre-, syn- and post-glacial processes occurring in the lacustrine basin during pre- and post-LGM times, (iii) determining the nature, origin, and age of an unreported, kilometre-scale, mound-field complex, by correlating the MCS data with lithological information from core Co1309, and finally, (iv) reconstructing the depositional, environmental and deglaciation history of the entire lake basin.

## 2. Site information

### 2.1. Geographical and geological setting

Lake Ladoga in NW Russia corresponds to the largest freshwater basin in Europe, both by its surface area and by volume; and serves as a freshwater reservoir for the city of St. Petersburg (Fig. 1). Lake Ladoga is ~220 km long, ~125 km wide and the area approximates 18,740 km<sup>2</sup> (Subetto et al., 1998; Naumenko, 2013). The modern lake surface reaches ~5 m above the sea level. The water depth is ~47 m in average, with the maximum water depth of ~235 m occurring in the northernmost part of the lake basin and the lake floor gradually shallowing towards the south (Fig. 1c) (Subetto et al., 1998; Naumenko, 2013, 2015). Direct precipitation, rivers and streams contribute to the recharge of the lake. In total, 35 inlets feed Lake Ladoga, with the Svir, Vuoksa and Volkov Rivers being the most important ones (Fig. 1b) (Subetto et al., 1998). The Neva River, located to the south, represents the only outlet currently present at Lake Ladoga, through which the lake discharges into the Gulf of Finland (Fig. 1b). The watershed area covers approximately 28,000 km<sup>2</sup>. The total catchment area, which includes the neighbouring basins of Lake Onega-Svir River (83,200 km<sup>2</sup>), Lake Ilment-Volkov River (80,200 km<sup>2</sup>), and Lake Saimaa-Vuoksa River (66,700 km<sup>2</sup>), plus several small riverine drainage areas sums up to ~258,500 km<sup>2</sup> (Fig. 1a) (Alekin and Smirnova, 1984; Rumyantsev and Drabkova, 2002).

Lake Ladoga is located at the border between the Fennoscandian crystalline Precambrian Baltic Shield (to the north) and the East European Platform (to the south), in an ancient tectonic depression named "Riphean graben syncline". This depression was subsequently reshaped by glacial erosion during the Quaternary (Subetto et al., 1998) and consists of metasediments, effusive and sedimentary rocks of Archean to Cambrian age covered by Quaternary deposits from the last glaciation (e.g. Subetto et al., 1998; Gromig et al., 2019). Post-glacial isostatic uplift is presently ongoing, with a higher rate in the northern lake basin (2.5 mm a<sup>-1</sup>) compared to the southern part (1.5 mm a<sup>-1</sup>) (Saarnisto, 2012).

### 2.2. Geomorphology of the lake floor and shorelines

From a compilation of few bathymetric maps available (e.g. Sorokin et al., 1996; Amantov, 2014; Naumenko, 2013, 2015, Fig. 1c), Anokhin et al. (2018) proposed a geomorphological map of the Ladoga lake floor. High reliefs, with vertical differences ranging from 100 to 200 m, forming linear, NW–SE-oriented structures, were reported in the northwestern part of the lake basin. Distinct channel- and ridge-like structures, along with steeply inclined slopes, were also recognized earlier in the northern basin by Subetto et al. (1998). In contrast, a smoother character of the lake floor has been highlighted in the southern region, with relief heights reduced to an order of magnitude (<10 m high) compared to its northern counterpart. Neither clear lineation nor orientation was denoted to the south. Three main zones were denoted by Anokhin et al. (2018): (i) the northern part, referred to as the

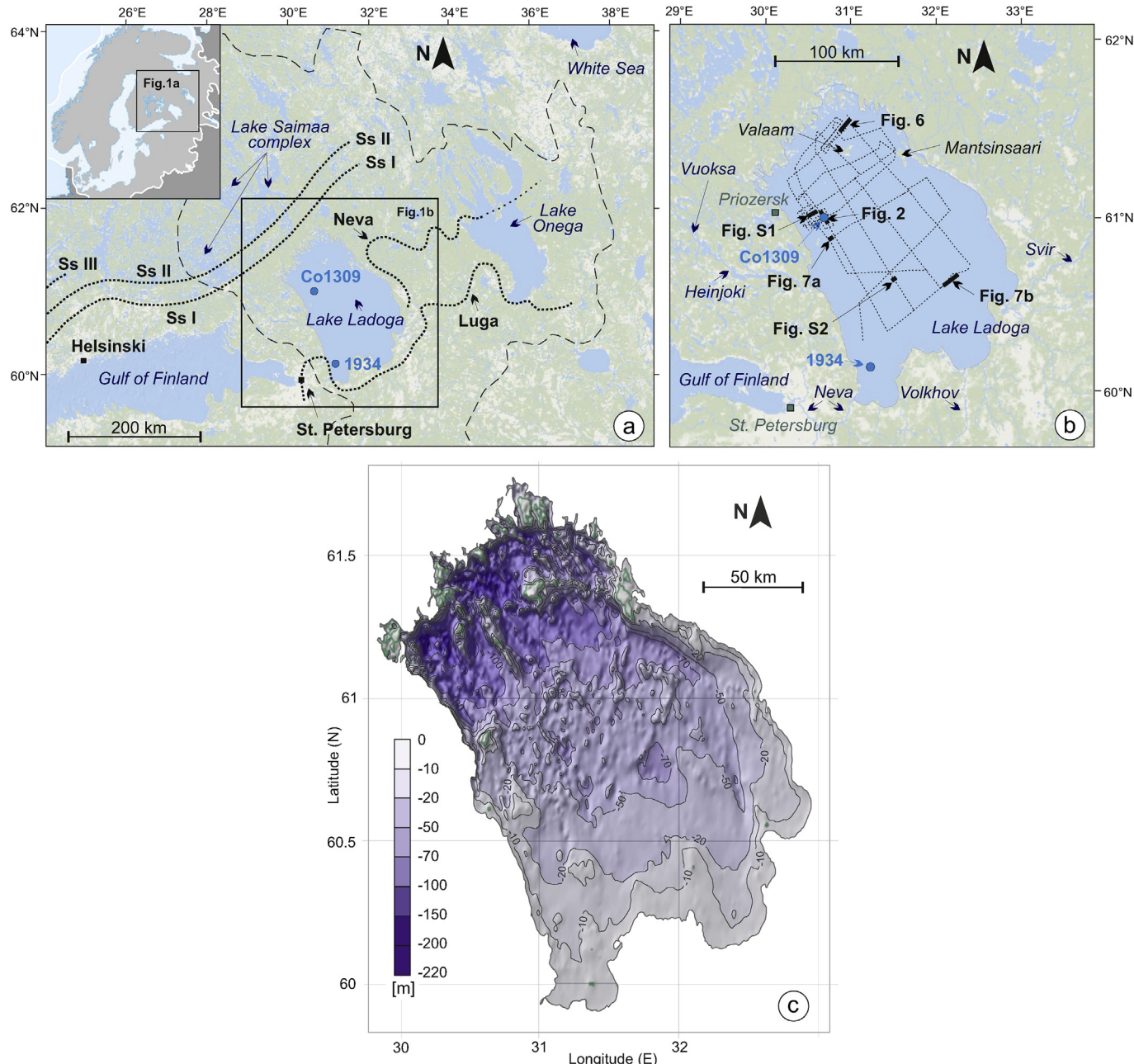


**Fig. 1.** (Inset) Regional overview of the study area. Thick white line represents the extent of the Scandinavian Ice Sheet during the LGM as portrayed by Stroeven et al. (2016). (a) Location of Lake Ladoga in NW Russia, with indication of the end moraines (dotted lines) encountered nearby (Luga, Neva, Salpausselkä (Ss) I, II and III), which marked the progressive retreat of the SIS during the LGM. Dashed line marks the present-day catchment area, which includes Lake Onega, the Lake Saimaa complex and Lake Ilmen (not shown here). (b) Enlarged view of Lake Ladoga, with indication of drainage network and main rivers (Svir, Vuoksa, Volkov and Neva). Dotted lines mark the location of the seismic data collected in 2013 using an airgun as well as the location of the Innomar echo-sounder data. Blue dot indicates the location of the sediment core Co1309 and '1934' recovered, respectively, in 2013 and 1934. Dark, bold lines correspond to the locations of the profiles illustrated in Figs. 2, 8 and 9. (c) Bathymetric contours of Lake Ladoga superimposed on a shaded relief map. (For interpretation of the references to colour in this figure legend, the reader is referred to the Web version of this article.)

structural-denudation area, with valleys and ridges related to the Baltic Shield Zone; (ii) the central region, regarded as an abrasive-accumulative zone; and (iii) the southern part, an accumulative zone made of plain deposits. The structural lineations reported to the north were regarded by the authors as potential sub-surface expressions of fault systems (Fig. 1c).

On land, NW-SE-oriented ridges resulting from the tectonic activity and glacial erosion are commonly found in the northernmost part of the catchment area along with glacial landforms such as eskers, kames and morainic hills formed during the LGM (Rumyantsev et al., 1999).

### 2.3. Regional glacial history

Lake Ladoga was affected by several glaciations during the late Quaternary, i.e., the Saalian glaciation (MIS 6; known in Russia as the Moscow glaciation; Malakhovsky and Markov, 1969; Svendsen et al., 2004; Maksimov et al., 2015) and the Last Glacial Maximum (LGM; ~20 ka; Svendsen et al., 2004). Traces of MIS6 have been identified near the town of Priozersk (NW shore; Fig. 1b) by the presence of two tills in borehole data. These tills contain high contents of sedimentary rocks and are separated by ~96-m-thick interstadial clays mostly of lacustrine origin (Malakhovsky and

**Markov, 1969**). Sediment cores retrieved on land in the southern part of the Ladoga area suggested the development of a large, freshwater lake during the last interstadial of the Saalian glaciation, so-called "Kaspilanskiy Interstadial" (Malakhovsky and Markov, 1969; Maksimov et al., 2015 and references therein). The following ice sheet that inundated the Ladoga region was the SIS during the LGM, which was less extensive than the Saalian glaciation. After the LGM, the deglaciation of the Ladoga basin and the formation of the lake itself took place during the so-called Neva stage, probably at ~14 cal ka BP (Gorlach et al., 2017). Investigations of new sediment core data acquired in the framework of the PLOT project allowed identification of three main recessional stages of SIS retreat from the Ladoga basin between 13.9 and 11.4 cal ka BP, with ice-margin oscillations between 13.2 and 12.3 cal ka BP (Gromig et al., 2019). The prominent Salpausselkä I (Ss I) and II (Ss II) end moraines located north of Lake Ladoga (Fig. 1a) marked the ice margin retreat of the SIS and, therefore, post-date the final deglaciation of the Ladoga basin (Saarnisto and Saarinen, 2001; Rinterknecht et al., 2006; Stroeven et al., 2016). According to cosmogenic  $^{10}\text{Be}$  exposure dating, Ss I was formed during the Younger Dryas (YD) at ~12.5 cal ka BP (Rinterknecht et al., 2004, 2006). A similar age was obtained by Gromig et al. (2019) who dated the Ss I formation at c.  $12.6 \pm 0.14$  cal ka BP. Following the retreat of the SIS, several local lakes formed in the southern region of the Ladoga basin (Ramsay, 1928; Markov and Poretzky, 1935; Kvasov, 1979). More importantly, Lake Ladoga became part of the Baltic Ice Lake (BIL) as a result of the SIS blocking the connection of the Baltic Sea basin to the North Sea basin (Björck, 1995; André et al., 2002). The drainage of the BIL resulted in a catastrophic flooding event into the North Sea at the YD (Björck, 1995; Jakobsson et al., 2007; Bennike and Jensen, 2013; Stroeven et al., 2015). This event, previously dated at 11.4–12.2 cal ka BP (Sauramo, 1958; Dolukhanov 1979; Donner and Raukas, 1992), was recently reassessed at  $11,620 \pm 100$  cal a BP by Stroeven et al. (2015).

#### 2.4. Lacustrine history of Lake Ladoga

Following the drainage of the BIL, the Ladoga basin remained part of the Baltic basin during the Yoldia Sea and Ancylus Lake stages, but it became isolated from the Ancylus Lake at c. 10 cal. ka BP (Saarnisto, 2012). At c. 9.5 ka BP (10.9 cal ka BP), the waters of the neighbouring Lake Onega drained into Lake Ladoga via the Svir River (Fig. 1b), which most likely strongly influenced the water level of Lake Ladoga (Saarnisto et al., 1995; Saarnisto and Saarinen, 2001). The newly isolated Lake Ladoga first drained towards the northwest into the Gulf of Finland via the Heinjoki threshold (Fig. 1b) (Ailio, 1915; Saarnisto and Grönlund, 1996; Dolukhanov et al., 2009, 2010; Subetto, 2009; Saarnisto, 2012). Ongoing regional postglacial isostatic uplift led to considerable changes in the hydrological system of Lake Ladoga and ultimately to the so-called Ladoga Transgression that caused a lake-level rise of about 10 m (i.e. >20 m a.s.l.; Saarnisto and Grönlund, 1996). At ~5 ka BP (5.7 cal. Ka BP), the waters of the lacustrine Saimaa complex (Fig. 1a) broke through the Ss I moraine and drained into the Ladoga basin (Saarnisto, 1970). This event increased the catchment of Lake Ladoga by 25% and caused a sudden rise of the lake level of 1–2 m (Saarnisto, 1970). Nonetheless, no clear evidence in the lake sediments supported these invasions (Davydova, 1985; Saarnisto and Grönlund, 1996). The Ladoga Transgression ended at ~3.35 cal ka BP, when the Neva River formed the modern outlet of Lake Ladoga at its southern shore (Fig. 1b) (Malachovskii et al., 1996; Dolukhanov et al., 2009, 2010; Saarnisto and Grönlund, 1996; Saarnisto, 2012). Simultaneously the lake level dropped significantly, with a lowering of ~12 m at Valaam Island (Fig. 1b) (Saarnisto, 2012) and 10–12 m in the southern part of Lake Ladoga

(Dolukhanov et al., 2009, 2010).

### 3. Data and methods

#### 3.1. Seismic acquisition and processing

The seismic data used in this study were acquired in August/September 2013 in the framework of the Russian-German project 'PLOT' (Melles et al., 2019). In total, ~1500 km of high-resolution, multi-channel seismic (MCS) profiles were acquired on Lake Ladoga (Fig. 1b), aboard the Russian R/V Poseidon. A small airgun (0.2 l) was used as a source and a 50 m-long, 32-channel Geometrics GeoEel digital streamer, with a channel spacing of 1.5625 m, as a receiver. Shot time interval was 4 s, corresponding to a distance of ~12 m at averaged survey speed. The dominant frequencies of the seismic signal were between 100 and 500 Hz. A GPS device was used for navigation, allowing a positioning accuracy of a few meters. More details about acquisition parameters are presented in Table 1.

Seismic processing was conducted with the Schlumberger Vista software© and included the following: geometry assignment, binning at 5 m, exponential gain correction, band-pass filtering (60–120–1000–1500 Hz), Surface Related Multiple Elimination (SRME), predictive deconvolution, Normal Move-Out (NMO) correction, stacking, and time migration using a constant velocity of  $1500 \text{ m s}^{-1}$ . The predictive deconvolution was applied to suppress the bubble pulse, which prevented a clear imaging of the real signal. As predictive deconvolution and SRME are time-consuming processing steps, they were only applied on a few selected lines that presented specific interests for this study. Hence, it is possible to see on a few seismic profiles a clear bubble pulse, often paralleling the strong reflection Sb2 (introduced thereafter), approximately 50 ms downwards.

Parametric sediment echo-sounder data were collected simultaneously to the MCS data using a SES-2000 device from Innomar. Thereby, the shallow subsurface of the lake floor has been captured down to ~35 m, with a vertical resolution in the decimetre range.

The IHS Kingdom software© was used for interpretation of both data sets. Prominent reflections (Sb1, Sb2, Sb3 and Sb4) have been mapped regionally (i.e. over the entire lake basin) (Figs. 2–7). To avoid uncertainties related to the large grid spacing of the data sets, sub-surface maps of these reflectors have not been generated. Thereafter, we express the thickness of the sequences (S) identified in the MCS data in meters, assuming a seismic velocity of  $1700 \text{ m s}^{-1}$  for the deeper sequences S1 and S2, and of  $1600 \text{ m s}^{-1}$  for the shallower sequences S3 and S4 (Krastel et al., 2017).

#### 3.2. Sediment coring and core processing

Subsequent to the seismic survey, a 22.75-m-long sediment core (Co1309) was retrieved in the northwestern part of Lake Ladoga, at a water depth of 111 m (Figs. 1 and 2) (e.g. Gromig et al., 2019). Coring was conducted from a floating platform (UWITEC Ltd.,

**Table 1**

Source and streamer characteristics of the 2D MCS data collected in 2013 on Lake Ladoga.

| Seismic source (type/volume) | small airgun 0.2 l |
|------------------------------|--------------------|
| Shot interval (s)            | 4                  |
| Streamer length (m)          | 50                 |
| Streamer # channels          | 32                 |
| Streamer group spacing (m)   | 1.5625             |
| Main frequencies (Hz)        | 100–500            |
| Survey grid (km)             | 1500               |

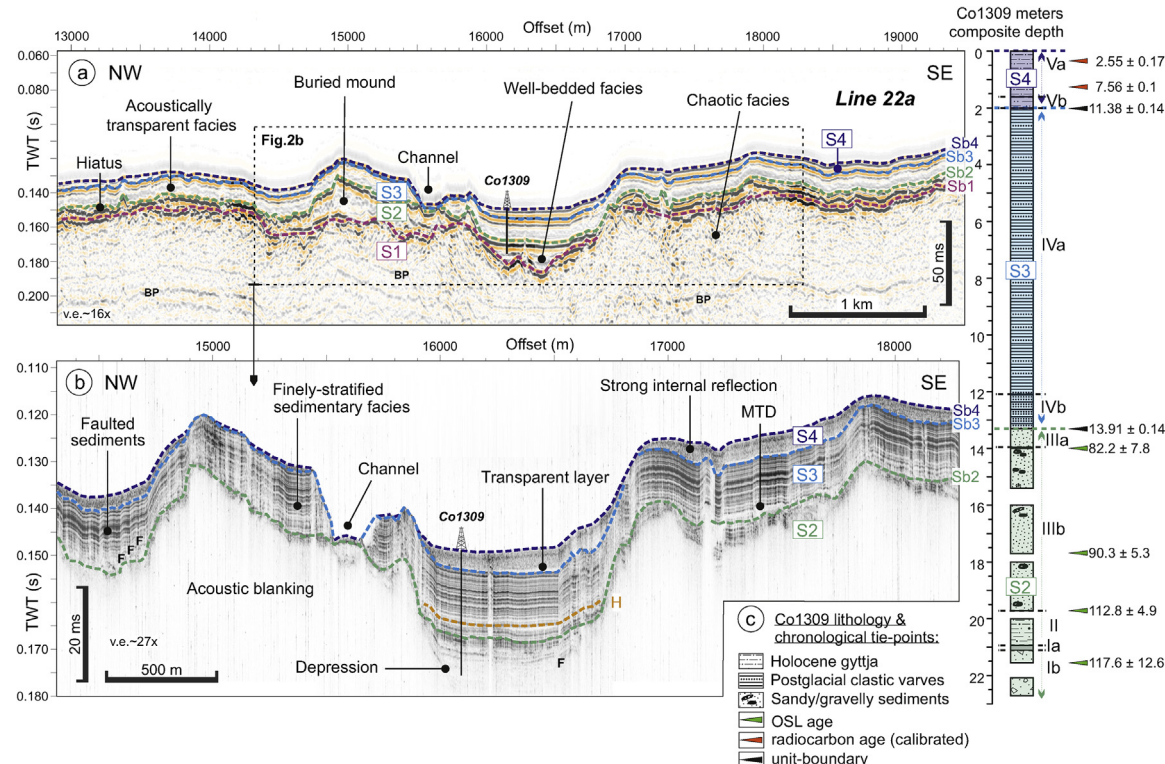


**Fig. 2.** (a) Illustration of the new, multi-channel seismic (MCS) reflection line 22a acquired in 2013, crossing the coring location at site Co1309 (for location see Fig. 1b). Four sequences (S1–S4) delineated by four prominent reflections (Sb1–Sb4) compose the lacustrine infill. Dashed, green line (Sb2) marks the location of the hiatus identified in core Co1309 between L2 IIIa and L2 IVb (Gromig et al., 2019), as shown in (c). BP = Bubble Pulse. (b) Enlarge view of the sediment echo-sounder profile 22a at site Co1309, for profile section see hatched box in (a). Finely-layered, well-bedded reflections define S3, while a semi-transparent facies characterizes the youngest sequence S4. TWT = Two-Way Travel times. F = Fault. v. e. = vertical exaggeration. The uneven morphologies of each reflection near site Co1309 (zigzag pattern) are due to strong wind effects during data acquisition. (c) Lithological column of core composite Co1309, ages and lithological zones (LZ I to V) as defined by Gromig et al. (2019) and Andreev et al. (2019). (For interpretation of the references to colour in this figure legend, the reader is referred to the Web version of this article.)

Austria), using a gravity corer to recover undisturbed surface sediments and a percussion piston corer to retrieve parallel, 2-m-long deeper sediment successions. The 2-m-long cores were cut into 1-m-long sections for transport.

Core Co1309 was extensively analysed using a multi-disciplinary approach. Chronological information is provided by varve counting as well as Optically Stimulated Luminescence (OSL) and radiocarbon ( $^{14}\text{C}$ ) dating (Gromig et al., 2019; Andreev et al., 2019). All calibrated ages that are related to the sediment core Co1309 have been calibrated with the intcal13 calibration curve (Reimer et al., 2013). Radiocarbon ages from the literature with no error bars have also been calibrated using the intcal13 calibration curve for comparison, and a range of calibrated ages have been provided next to the initial ages. The upper part of the core was additionally investigated for varve thickness, grain size, water content and chemical composition (Gromig et al., 2019), for pollen (Savelieva et al., 2019) and for biogenic silica contents and diatom isotopes (Kostrova et al., 2019). Complementary analyses in the lower part of the record concern lithology and pollen (Andreev et al., 2019).

#### 4. Late Quaternary seismic stratigraphy

The MCS and echosounder data collected in 2013 capture, for the first time, the lacustrine infill of Lake Ladoga in unprecedented detail, up to its basement. The roughly NW-SE and NE-SW orientated grid (Fig. 1b) reveals a detailed image of the structure and stratigraphy of the lacustrine basin, with a vertical resolution of a few meters for the MCS data and ca. 15 cm for the echosounder

data. Following the concept of Mitchum et al. (1977), four major sequences (S) were defined based on their internal reflection character, seismic facies and unconformities (Figs. 2–7). These sequences have been labelled, from bottom to top, S1 to S4. In attempt to define the nature, origin and age of each sequence, we correlated the MCS and hydro-acoustic data with the lithologies recovered at the coring site Co1309 (Figs. 1 and 2).

##### 4.1. Sequence S1

The sequence S1 is the oldest one captured by the MCS system, which most likely represents the bedrock (Figs. 2a, 3 and 4a,c,d, 6a). S1 displays a large variety of seismic facies, with well-bedded, sub-horizontal and sub-parallel reflections of low to moderate amplitude in some areas (Figs. S1, 3b). On most profiles, however, S1 is composed of gently-to steeply-dipping reflections of low to high amplitude, dipping in different directions and at different angles, locally faulted and/or folded (Figs. 3a and 4a,c,d). In exceptional cases, S1 presents a chaotic facies of low to moderate amplitude, such as near coring site Co1309 (Fig. 2a) and in areas where major faults crop out on the lake floor (Fig. 6a). Changes in seismic facies occur over short distances underlining a complex sequence formation and deformation history (Fig. 3a). Unfortunately, S1 was not recovered by core Co1309. Constraining the nature and age of the sequence would, thus, require further investigations using coring and drilling techniques at different locations. As the basal age of Co1309 is referring to the late Eemian interglacial (MIS 5e; in Russia known as Mikulino) (e.g. Andreev et al., 2019), S1 must be older. Finally, the top boundary of S1 is marked in the MCS data by a

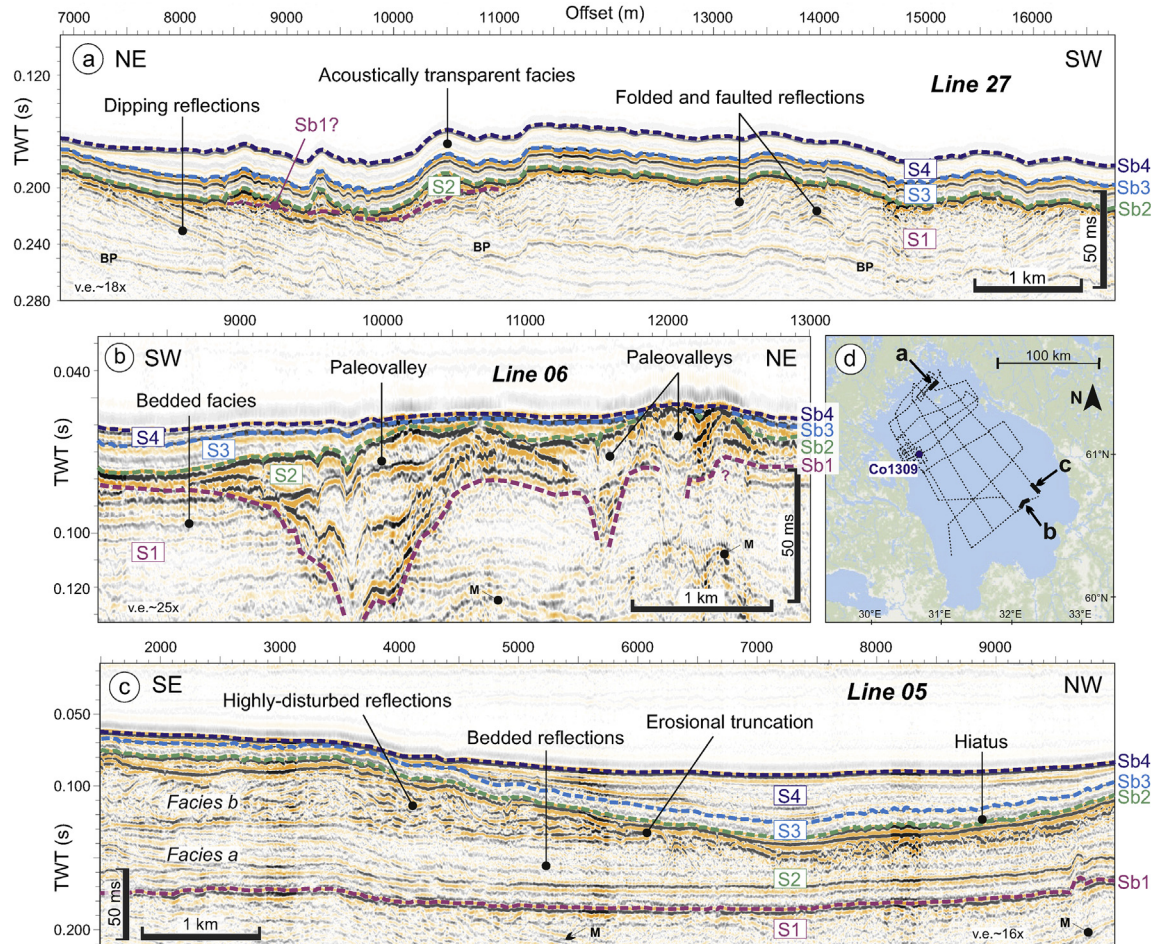


**Fig. 3.** (a) NE-SW seismic line 27 acquired in the northernmost region of Lake Ladoga, particularly imaging the oldest sequence S1, which shows folded and faulted strata. The hiatus delineated by Sb2 strongly truncates S1-sediments. S2 is solely represented here by Sb2 and two small mounds. (b) SW-NE seismic line 06 illustrating the paleo-glacial valleys encountered in Lake Ladoga and associated with the LGM, and, (c) SE-NW seismic line 05 showing a well preserved, ~90-m-thick remnant stratigraphy of S2 in the southernmost lake region. S2 is composed of two facies (*a* and *b*), which are progressively eroded north-westwards by Sb2. Note the continuity and very good preservation of the prominent reflection Sb1, which marks the upper boundary of the oldest sequence S1. v. e. = vertical exaggeration. M = Multiple. BP = Bubble Pulse. (d) Location of the seismic lines shown here (dark bold lines).

prominent reflection, thereafter referred to as Sb1 (Figs. 2a, 3, 4a,c,d, 6a). Mapping Sb1 was challenging, as the reflection has been strongly affected and eroded by subsequent geological processes (Figs. 3a,b and 6a). In places, paleovalleys (described in 4.1.2.) carved S1 (Fig. S1).

#### 4.2. Sequence S2

The overlying sequence S2 is by far the most interesting and complex sequence imaged in the MCS data (Figs. 2a, 3 and 4, 6a). In the echo-sounder data, only the uppermost meters have been imaged (Figs. 2b, 5a,b,d and 7a). Where captured, S2 may display well-bedded, finely-layered reflections of variable amplitude (Figs. 2b, 5a,b,d and 7a), reaching up to ~15 m in thickness in a few areas (Fig. 5a). In other areas, this layering is blurred (Fig. 4b) or replaced by a high-amplitude reflection (Fig. 5c). This highly-reflective character is punctually disrupted by acoustically transparent facies that carve into the sediments (Fig. 5a, b, d). Most of these features present an asymmetrical V shape of variable depths and are particularly common in the southern region, where they are often stacked (Fig. 5b, S2). Thin, transparent lenses intercalate within S2-sediments (Figs. 2b and 4b) and normal faults cutting through S2 are also observed in places (Fig. 5a, c, d, 6, 7). Despite the

presence of well-bedded reflections, S2 is predominantly characterised in the echo-sounder data by large blanking zones (Figs. 2b, 4b, 5 and 7), which correlate to large mounds in the MCS data (Fig. 4a,c, d). Near the shorelines, however, these blanking areas are often associated with former platforms.

The mounds imaged in the MCS data – outcropping on the lake floor or buried under subsequently deposited S3 and S4 sediments – display a wide variety of morphology, size, and internal architecture, which vary laterally along a profile and within the lake basin (Figs. 4 and 7). Fig. 4 illustrates this variety. The mound's dimension varies considerably, with lengths between hundreds of meters and several (up to 8) kilometres, and heights from <10 m to 170 m in the northernmost region. The partial coverage of the data set does not allow for an exact characterization of the mounds dimension and morphology. Therefore, it is possible that the mounds may reach higher lengths and heights than mentioned above. The mounds internal architecture is also complex and varies remarkably over the basin. Fig. 4a, for instance, illustrates two types of mounds encountered on Lake Ladoga. While the mound in the SE shows an overall conical shape, with two distinct reliefs, the mound in the NW rather contrasts to it by its overall smoothed, sub-rounded morphology. The mounds are ~3 km and ~2.3 km long, and ~69 m and ~53 m high, respectively. The SE-mound is mainly

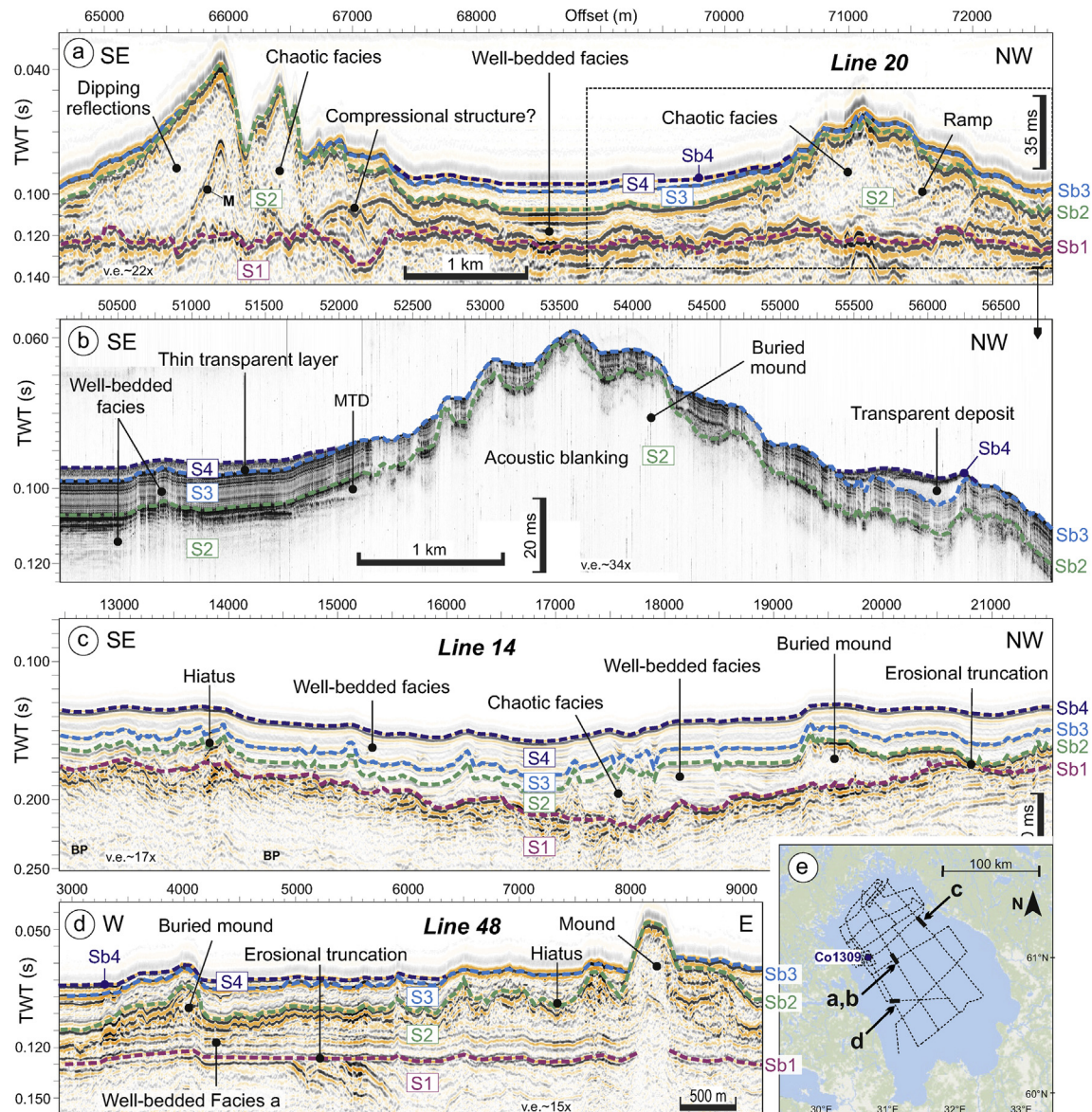


**Fig. 4.** (a) SE-NW seismic line 20 illustrating two different types of kilometre-scale mounds identified in Lake Ladoga. Mounds internal architecture has been captured in unprecedented detail in the MCS data, whilst acoustic blanking characterizes the mounds in the echo-sounder data (b). Sb1 and Sb2 mark, respectively, the lower and upper boundaries of each mound. (b) Enlarged view of the northwestern mound identified in (a) as captured in the echosounder data. (c) SE-NW seismic line 14 westwards from Mantsinsaari, showing an up to ~25-m-thick and undisturbed, stratified sediments that mostly compose S2; hence, contrasting with its usual appearance (i.e. mounds, few contorted reflections or merely Sb2). (d) W-E seismic line 48, showing the well-preserved, remnant stratigraphy of the sequence S2. Note the progressive erosion of S2 towards the west as well as the formation of a moraine mound to the east in S2 uppermost section. v. e. = vertical exaggeration. M = Multiple. BP = Bubble Pulse. (e) Location of the seismic lines shown here (dark bold lines).

made of well-bedded and parallel, dipping reflections of low-to moderate-amplitude, while a concave-downward prominent reflection is observed to the NW at the base of the mound (Fig. 4a, to the left). Two main facies characterise also the NW-mound, i.e., gently dipping, parallel reflections of moderate amplitude (to the NW), which are overlain by a low-amplitude chaotic facies to the SE (Fig. 4a, to the right). Stratified, ~15 m thick sediments separate the two mounds over hundreds of meters (Fig. 4a).

Westwards from Mantsinsaari Island (Fig. 1b), up to ~25 m-thick undisturbed, stratified sediments with low to medium amplitude reflections – exceptionally – compose the sequence S2 (Fig. 4c). Two small-scale, buried mounds, however, are present to each side. Such a thick and well-preserved sedimentary succession in proximity of mounds has only been observed in this area. Two

prominent reflections, thereafter referred to as Sb1 and Sb2, respectively mark the lower and upper limits of the mounds; consequently, of S2. It is worth reporting that both reflectors have an erosional/truncating character that affected the underlying sequence S1 (Figs. 3a,c, 4a,c,d, 6a). In contrast to Sb1, mapping of Sb2 was less challenging and successful throughout the entire basin.

#### 4.2.1. Remnant stratigraphy and paleovalleys

A relatively well-preserved, ~90-m-thick sedimentary succession has been imaged in the southwesternmost part of the lake basin (Figs. 4d and 3c). This succession is bounded at its top and base, respectively, by Sb2 and Sb1 and, therefore, belongs to S2. Such a discovery is quite unexpected, as most of S2 either consists

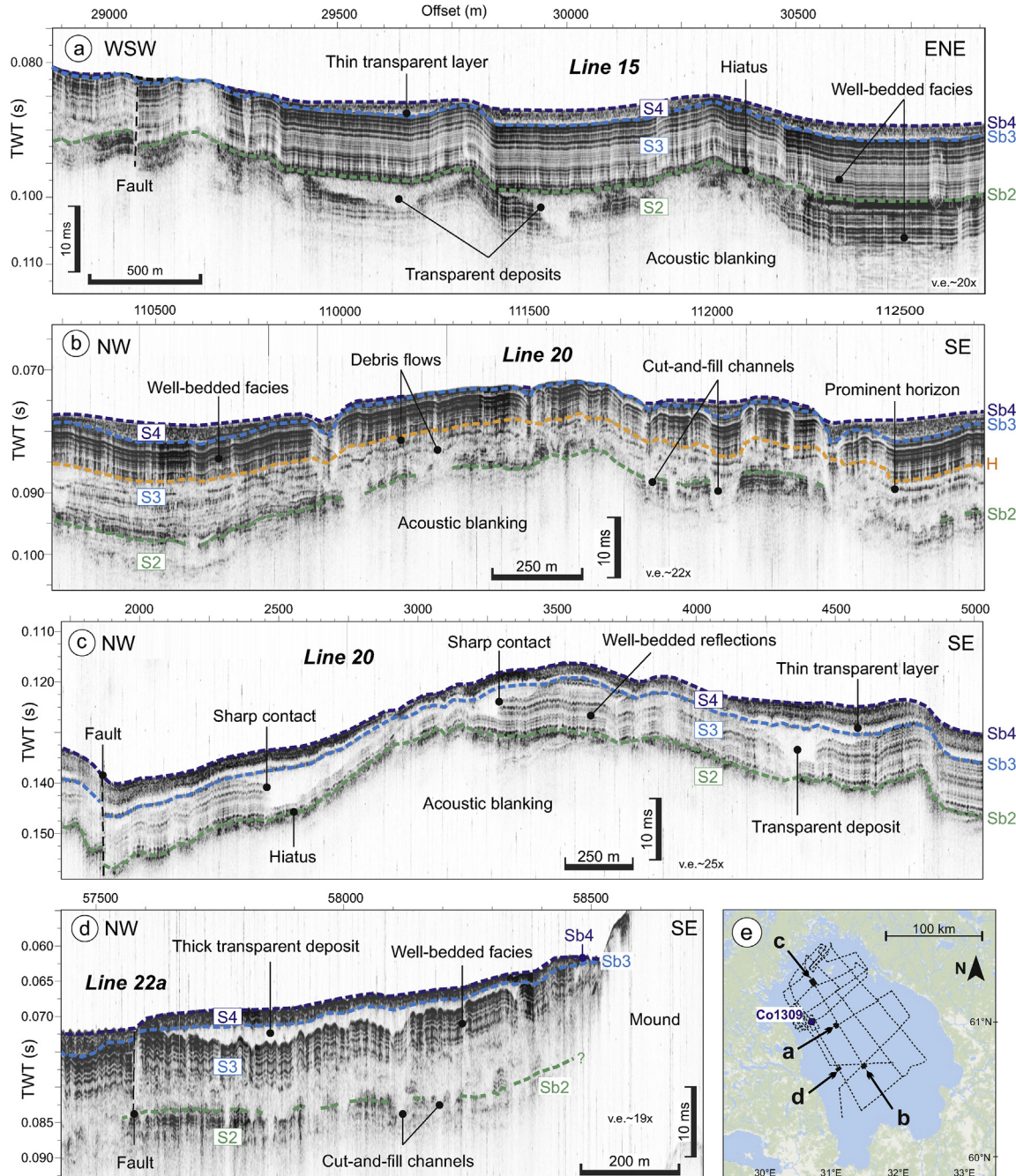


**Fig. 5.** (a) WSW-ENE echo-sounder line 15 and (b/c) NW-SE echo-sounder line 20, and (d) NW-SE echo-sounder line 22a showing the detailed signature of the sequences S2 to S4. The oldest sequence S1 has not been captured by the echo-sounder data. Numerous cut-and-fill channels, often stacked, affected the uppermost part of S2 over variable depths as shown in (a), (b), (d). These erosive features are regarded as resulting from sudden and intense meltwater discharges of the SIS during its overall retreat from the Ladoga basin. Elongated, transparent deposits identified in the lowermost part of S3, separated by prominent reflections, are interpreted as debris flows resulting from different contemporaneous meltwater pulses (b). Despite these punctual deposits, S3 displays its usual acoustic signature (i.e. finely-layered, well-bedded reflections). Erosive, transparent deposits affecting the uppermost section of S3 are also noted in (c), which contrasts with the non-erosive, transparent deposits imaged in (d). Note the flat morphology of these deposits that are also regarded as debris flows. v. e. = vertical exaggeration. F = Fault. (e) Location of the seismic lines shown here (dark bold lines). The uneven morphologies of each reflection in (c) and (d) (zigzag pattern) are due to strong wind effects during data acquisition.

of (i) large-to small-scale mounds (Figs. 2a, 4, 5d and 7), (ii) few contorted reflections delineated by Sb2 and/or Sb1 (Fig. 2a), or (iii) only represented by Sb2 (Figs. 2a, 3a and 6a). The sedimentary succession is made of a seismic *Facies a* in its lowermost part that is composed of well-bedded, sub-horizontal to slightly dipping, low-to moderate-amplitude reflections (Figs. 3c and 4d); and of a seismic *Facies b*, in its uppermost part, consisting of contorted to

slightly chaotic, moderate-to high-amplitude reflections (Fig. 3c).

The MCS data also image a few large paleovalleys, falling in the range of up to 5 km width, and around one hundred meters depth that carve into S1-sediments (Fig. S1). In seismic line 34, the paleovalley is ~4.9 km wide and at least ~135 m deep (between offsets 5700–10,700; Fig. S1). The acoustic signature of the upper section is characterised by sub-horizontal, parallel, well-bedded

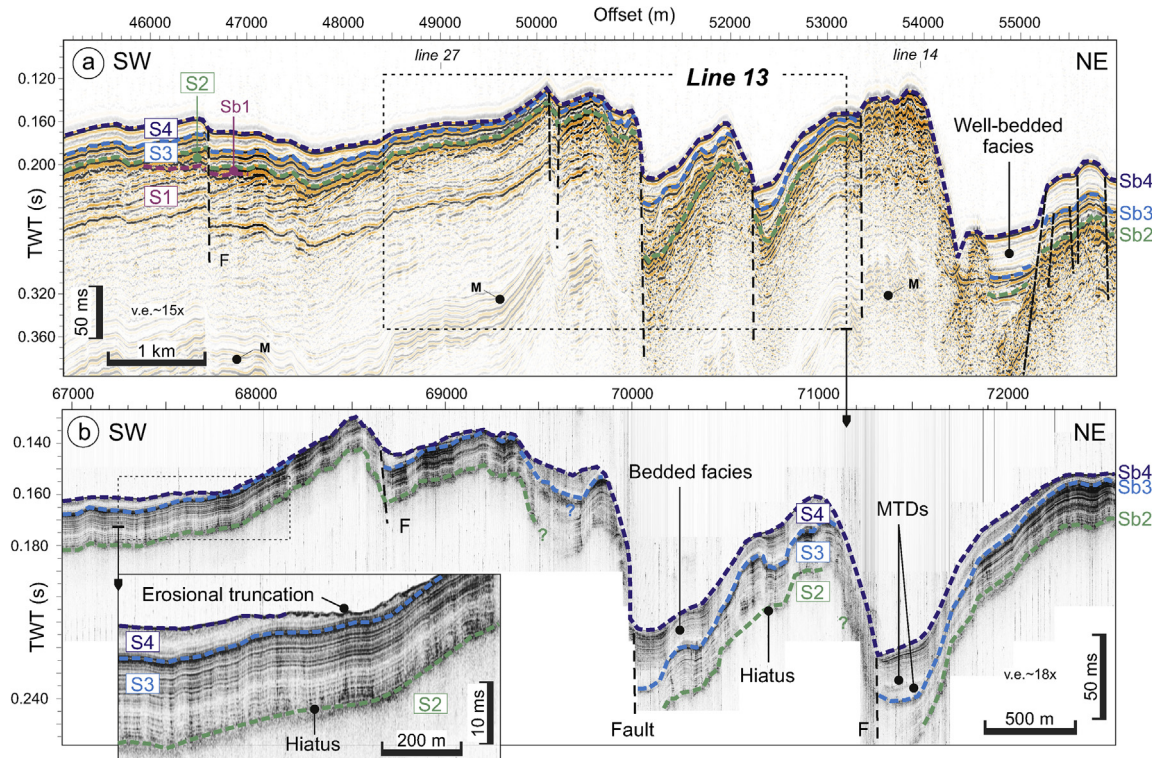


**Fig. 6.** (a) SW-NE seismic line 13, illustrating the major, normal fault systems affecting the northernmost part of Lake Ladoga (for location see Fig. 1b). (b) Enlarged view of line 13 showing the acoustic signature of S2 to S4 in the tectonically active area. Inset shows the blurry character usually identified in the echo-sounder data for the hiatus (Sb2) and illustrates recent erosion affecting the youngest sequence S4. Prominent reflections are interpreted as made of coarser-grained material that accumulates under shallower lake-water level conditions. v. e. = vertical exaggeration. M = Multiple. F = Fault.

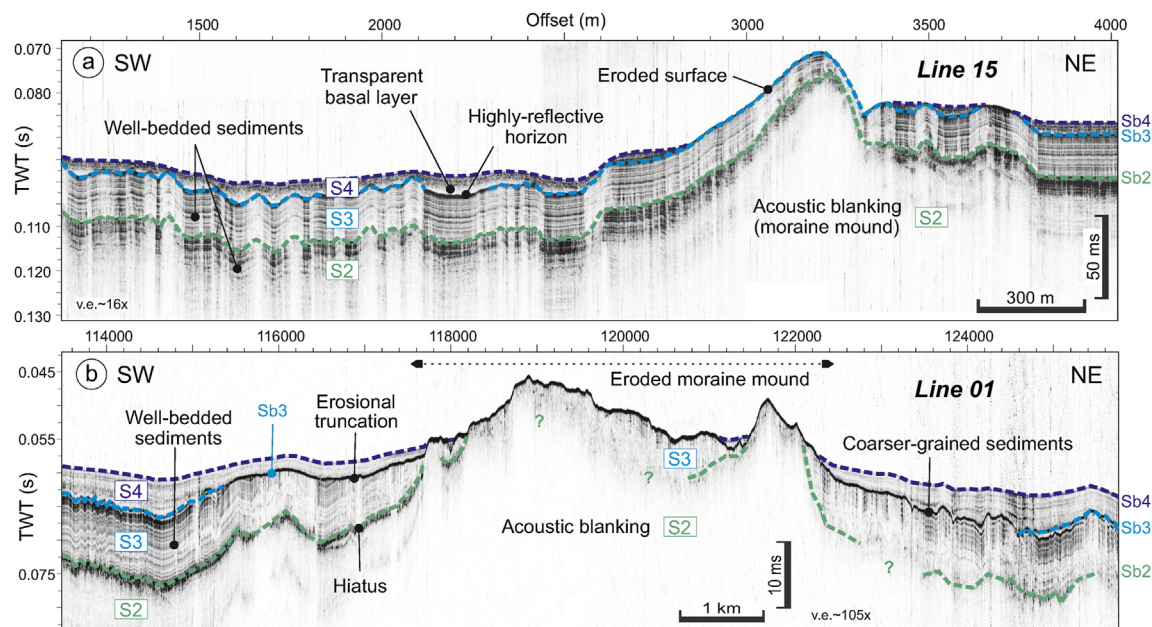


**Fig. 7.** (a) SW-NE echo-sounder line 15, illustrating the unusual, thick and dark acoustic signature of the top boundary of S3 near the western shoreline. This prominent reflection conformably drapes S3-sediments to the outcropping mounds, where it truncates S3. The very dark reflection is interpreted as made of coarser-grained material that accumulated during a lowering of the lake level after the drainage of the BIL. Note the thin, transparent layer overlying this reflection at the base of S4. (b) SW-NE echo-sounder line 01 showing the remodeling of a large-scale mound in the southern region, likely due to several lake level drops, which led to the formation of the very dark and thick prominent reflection as noted in (a). A truncation of S3-sediments by this reflection is clearly seen here. For location of profiles 15 and 01, see Fig. 1b v. e. = vertical exaggeration.

reflections of variable amplitude, which onlap onto the WSW wall of the paleovalley. These bedded reflections correspond to the seismic *Facies a*, which defines the lowermost part of S2. To the ENE, in contrast, contorted reflections of moderate amplitude define the infill (Fig. S1) and highly resemble the ones composing the buried, lens-shaped mound identified to the ENE. Due to limited signal penetration, the acoustic signature of the deepest part could not be resolved. Such large paleovalleys seem to be restricted to the western part of the lake, up to 35 km from the shoreline, but we cannot exclude that this restriction may be due to the partial coverage of our data set.

Smaller paleovalleys, with width falling in the range of 600 m to 1.5 km and over ~10 m–60 m deep, have also been observed and rather present a wider variety of morphology and fill (Fig. 3b). In seismic line 06, for instance, the valley is ~1.9 km wide and ~62 m deep, and displays a pronounced V shape (Fig. 3b). Four prominent reflections presenting small to large V-shaped indentations separate three distinct fills, which mark different aggradational stages in the valley development. Such paleovalleys are located predominantly close to the southern and northwestern shorelines. Interestingly, the prominent reflection Sb2 caps most of the paleovalleys identified in the MCS data.

#### 4.2.2. Seismic-to-core correlations

Correlating the hydroacoustic data to sediment core shows that only the uppermost part of S2 has been sampled at site Co1309; which corresponds to the lowermost 9.45 m composite depth (c.d.) of the retrieved sediments (Fig. 2c). From bottom to top, these sediments consist of (i) fine-to coarse-grained sand with pebbles of different lithologies, including granitic, dark metamorphic and sandstone pebbles (from 22.75 to 21.25 m c. d.; lithological zone LZ Ib), (ii) silty clay intercalated with sand layers (from 21.25 to 20.95 m c. d.; LZ Ia), (iii) sharp-laminated silty clay with fine-to coarse-grained sand (from 20.95 to 20 m c. d.; LZ II), and (iv) well-sorted, fine to medium sand with clays and sporadic coarse-grained sand lenses (from 20 to 14 m c. d.; LZ IIIb) and without lenses (from 14 to 13.30 m c. d.; LZ IIIa; e.g. Andreev et al., 2019). To simplify, S2 is mostly characterised by a variety of lithologies that consist of alternating sand and clay to silt layers.

OSL ages and pollen stratigraphy indicate that the entire sediment succession (from 22.75 to 13.30 m c. d.) was deposited during MIS 5, presumably from the Eemian interglacial (MIS 5e) to the Middle Weichselian (MIS 5a; known in Russia as Middle Valdai) (e.g. Andreev et al., 2019). Noteworthy is the evident correlation of the sand layer LZ IIIa (Fig. 2c) with the prominent reflection Sb2, which marks the upper limit of S2; therefore, of the mounds (e.g. Fig. 4). According to the age model of core Co1309 there is a hiatus of ~60 ka between LZ IIIa and the overlying LZ IV-sediments (e.g. Gromig et al., 2019), i.e. at reflection Sb2 (Figs. 2–7).

#### 4.3. Sequence S3

The sequence S3 overlies and conformably drapes S2-sediments. In the MCS data, S3 is characterised in its lower part (~ $\frac{2}{3}$  thickness) by continuous, well-bedded, low-to moderate-amplitude reflections, while a prominent reflector, referred to as Sb3, defines its upper section (~ $\frac{1}{3}$  thickness) (Figs. 2a, 3 and 4, 6a). In general, the sequence shows a constant thickness within the lake basin of ~9 m. However, near the mounds that crop-out on the lake floor, S3 thins drastically to a few meters while it is usually absent on top of those (Fig. 4a,b,d, 5d, 7). In channel areas (Fig. 2) and near the shorelines, where past lake-level variations most likely truncated the sequence, S3 may be partially to entirely eroded (Figs. 3b and 7b). On the other hand, S3 conformably drapes buried mounds (Figs. 2a, 4c and 7a).

The echo-sounder data provide further information concerning the internal architecture of S3. Typically, the sequence is characterised by finely layered, closely-spaced reflections of variable amplitude (Figs. 2b, 4b and 5, 6b, 7, S2). This signature varies along the profiles and within the basin. In line 15, for instance, it is possible to subdivide S3 into three parts of similar thicknesses (Fig. 5a). While the lowermost part alternates between high-, low- and moderate-amplitude reflections, the central part shows much thinner layers of sediments of low to moderate amplitude, which strongly contrasts with highly-reflective and thick horizons in the upper part. Erosional unconformities truncating S3 are documented near the shorelines of the eastern, western (Fig. 7a), northern (Fig. 6b) and southeastern (Fig. 7b) lake. In areas, where S3 has been heavily eroded, a highly-reflective horizon caps the fine laminations (Figs. 6b and 7).

Massive transparent bodies are also observed in the uppermost sequence section, in the northern, western and eastern regions. Most of these bodies truncate S3-sediments (Fig. 5c), but some accumulated conformably onto the sediments (Fig. 5d). These transparent bodies are up to 7.5 m thick and 600 m long, and display a flat shape at their top boundary. V-shaped and lens-shaped, transparent features have also been locally imaged near the sequence base (Figs. 2b and 5d). Interestingly, these transparent features disappear along a specific stratigraphic surface that we refer to as 'H' (Fig. 5b). Finally, it is worth noting that the sequence S3 appears heavily fractured and faulted in several places, more frequently and abundantly than its counterparts S1, S2 and S4 (Fig. 7).

Correlating the sequence S3 with sediment core Co1309 (e.g. Gromig et al., 2019) shows that S3 coincides with the lithological zone LZ IV (from 13.30 to 2.02 m c. d.; Fig. 2c), which consists of finely-laminated couplets of variable thickness (1–35 mm) of bright sand or silt at the base and dark grey clay layers at the top. These finely-laminated sediments have been interpreted as clastic varves by Gromig et al. (2019). The laminated character of LZ IV has been particularly well captured by the echo-sounder data and represents the main acoustic signature of S3 (Figs. 2b, 4b, 5 and 6b, 7). Few coarse-grained, sandy sediments were noted at the base of particularly thick and coarse-grained varves, as well as at the base of more thick graded layers that were interpreted as turbidites (Gromig et al., 2019). Varve chronology derived from core Co1309 indicates a deposition of LZ IV-sediments and, therefore, of S3, from  $13,910 \pm 140$  to  $11,380 \pm 140$  cal a BP (Fig. 2c), with a resultant mean sedimentation rate of  $4.4 \text{ mm a}^{-1}$  (Gromig et al., 2019).

#### 4.4. Sequence S4

The uppermost sequence S4 is characterised in the MCS data by low-to moderate, continuous and well-bedded seismic reflections (Figs. 2a, 3 and 4, 6a). The sequence mostly draped S3-sediments giving the lake floor an inherited morphology (Figs. 3a, 4b, 5c-d). In some areas, however, S4 fills and onlaps pre-existing lows associated with the uneven morphology of buried mounds (Fig. 4a).

In the echo-sounder data, S4 is mainly characterised by a semi-transparent facies (Figs. 2b and 5a/c, 6 b, 7a). Few bedded reflections are, nonetheless, noticed in places (Fig. 5a). Near the southeastern shoreline, only well-bedded, sub-parallel reflections of low to moderate amplitude characterise S4 (Fig. 7b). These reflections are truncated at their top by a highly-reflective horizon (Figs. 6b and 7b). Highest thicknesses are reached near the northeastern and northern shorelines, with up to 20 m as compared to a mean thickness of ~10 m. A thin, transparent layer covers the base of S4 in several places (Figs. 2b, 4b, 5a/c, 6b and 7) and shows a variable thickness. A prominent reflection separates this transparent cover from the large S3-transparent bodies (Figs. 5c and d,

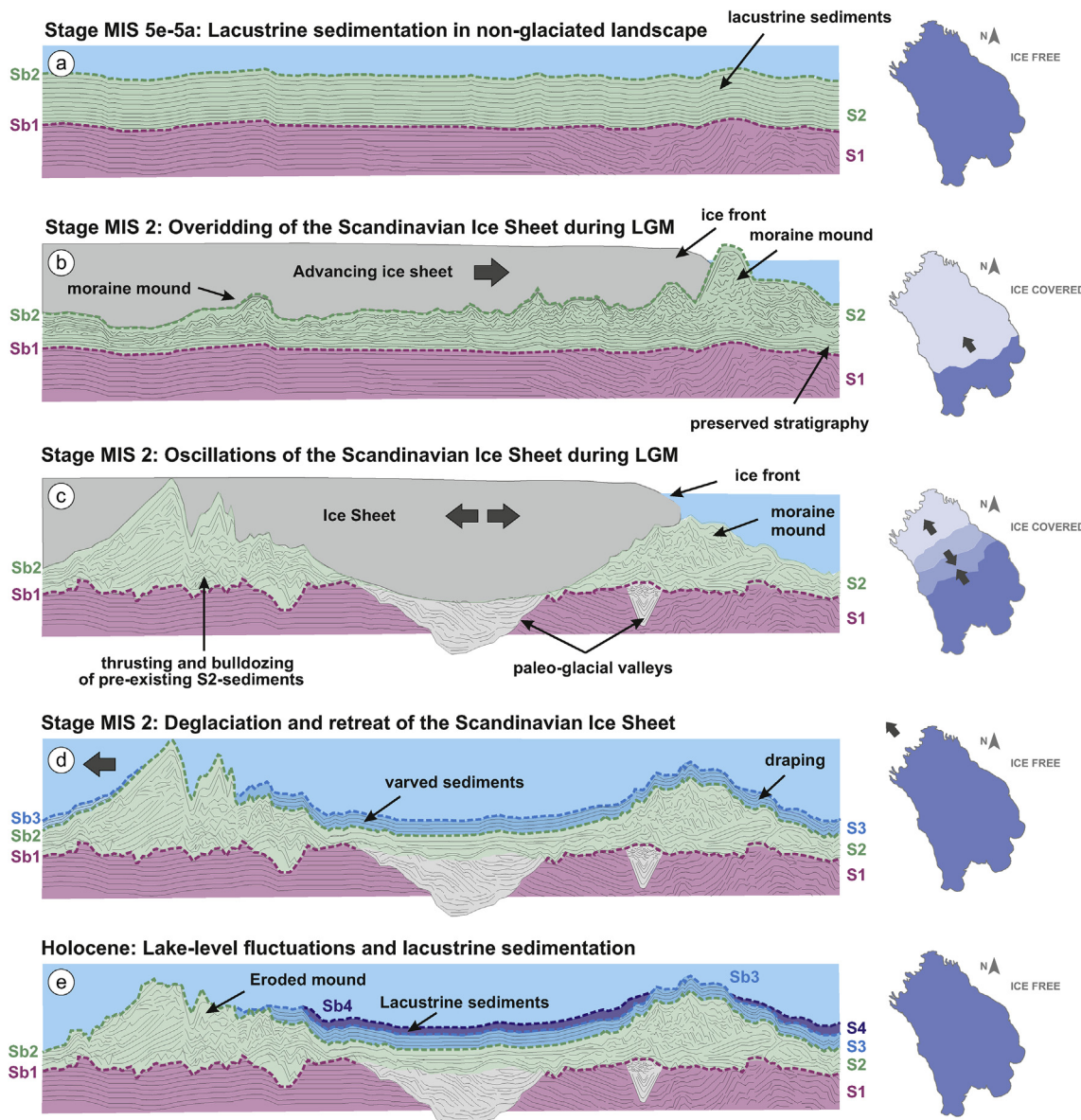


**Fig. 8.** Conceptual landscape model of Lake Ladoga basin showing the stratigraphic evolution of the lacustrine infill.

6b, 7). Similar to S3, S4 thins drastically and partly disappears on the mounds that crop-out at the lake floor (Figs. 4a, 4b, 4d and 7). As for its counterparts S2 and S3, normal faults offset the unit by few meters (~10 m) in the northernmost region (Fig. 6).

Correlations of the hydroacoustic data with sediment core Co1309 indicates that the sequence S4 consists of a gyttja that can be separated into (i) massive silty clay of olive grey to very dark greenish grey colour with intense bioturbation, which suggests oxygenation of bottom waters (from 2.02 to 1.60 m c. d.; LZ Vb; Fig. 2c) and (ii) well-stratified clayey silt of dark greyish brown colour with brownish and greenish to blackish layers, with deposition of ice-raftered debris (IRD) more frequent than in LZ Vb (uppermost 1.60 m c. d.; Fig. 2c; e.g. Gromig et al., 2019). Maximal water-contents occur in the near-surface sediments, reflecting minimal compaction. This high-water content most likely confers S4 semi-transparent character as imaged in the echo-sounder data (Figs. 2b, 5a/c and 6b, 7a).

The age-depth model (e.g. Gromig et al., 2019) indicates an age

from  $11.38 \pm 0.4$  cal ka BP until today for the deposition of LZ V-sediments and therefore, for S4 (Fig. 2c). This reflects an average sediment rate of  $0.18 \text{ mm a}^{-1}$ , which is ~24 times lower than that during the formation of S3.

## 5. Discussion: history of Lake Ladoga

### 5.1. Sedimentary processes and depositional character

#### 5.1.1. Lacustrine bedrock

The deepest sequence S1 presents a wide variety of seismic facies that attests to a complex history of formation and deformation. Determining the nature, age and origin of S1 appears difficult, as no cores have as yet sampled the sequence, including core Co1309 (Fig. 2). From its seismic signature it is suggested that S1 represents the bedrock of the lacustrine basin. If so, it likely consists of metasediments, effusive and/or sedimentary rocks of Archean to Cambrian age (e.g. Subetto et al., 1998; Amantov, 2014).

### 5.1.2. Moraine mounds

The lithological information retrieved at site Co1309 (Figs. 1 and 2), shows that the upper section of S2-sediments cover the time-frame from MIS 5e to MIS 5a (Andreev et al., 2019) (Fig. 8a). Sedimentological and palynological investigations also underlined a hiatus of more than 60 ka between the non-glacial sediments (LZ IIIa) and the overlying varves (LZ IV) (Fig. 2c). This hiatus was attributed by Gromig et al. (2019) to the overriding of the SIS during the LGM that could have eroded pre-existing sediments and deposited sand (LZ IIIa; Fig. 2c) instead of a till as it has been typically found in the region (e.g. Bakhmutov and Zagniy, 1990; Saarnisto et al., 1995; Saarnisto and Saarinen, 2001) or in the Baltic Sea (e.g. Andrén et al., 2015). This hiatus coincides well with the reflection Sb2 in the MCS data (Figs. 2a, 3 and 4, 6a) allowing us to interpret Sb2 as marking the overriding of the SIS in the lacustrine infill (Fig. 8b). Thus, we interpret the mounds captured in S2 (Fig. 4) as being mostly made of MIS 5e/MIS 5a-sediments or older ones than those retrieved at site Co1309, as S2 only represents there a few percentages of the whole sequence as captured in the MCS data (Figs. 3c and 4d). As Sb2 also eroded Sb1 in many areas (Figs. 3a/b and 6a), it is likely that some of the mounds also incorporated S1-material in variable proportions.

Sublacustrine landforms forming ridge-like structures have been reported by Amantov (2014), Amantov and Amantova (2014) and Anokhin et al. (2018) in the northwestern and central parts of Lake Ladoga (Fig. 1c). To the north, these landforms were regarded as ridges associated with the Baltic Shield Zone. In the central region, abrasive-accumulative processes were thought to have built these landforms, but their nature, age and responsible geological processes were not determined. The mounds imaged in the MCS data (Fig. 4) could correspond to some of the landforms described by Amantov (2014), Amantov and Amantova (2014) and Anokhin et al. (2018), however, the lower resolution of the bathymetric data available on Lake Ladoga hampers such a correlation (Fig. 1c). Nevertheless, the metric-scale resolution of our MCS data, along with coring information at site Co1309, allowed us to investigate the nature, age and origin of these mounds, for the first time.

The mounds captured on Lake Ladoga highly resemble moraine mounds reported in the White Sea (Rybalko et al., 2018) and terrestrial moraine-mound complexes evidenced in Svalbard, Scotland and Britain (Hambrey et al., 1997; Graham and Midgley, 2000). These complexes, frequently referred to as "hummocky moraines" (i.e. irregular mounds of glacial debris), were first interpreted as the product of down-wasting of stagnant ice as a result of a rapid cessation of the glacier activity in response to sudden climate ameliorations (Sharp, 1949; Sissons, 1980). Work on modern glaciers, however, suggested that these moraine-mound complexes more likely are the result of thrusting in glacier ice and in the proglacial sediments. From detailed observations of the sedimentary facies, structure and morphology of such moraine-types in Svalbard, Hambrey and Huddart (1995) interpreted these mounds as the product of thrusting of subglacial material into an englacial – occasionally supraglacial – position, prior to melting out. Moreover, the authors reported that the mounds exposure was the result of an ice margin, up-valley recession rather than glacier stagnation. The Ladoga mounds bear strong similarities with the moraine-mound complexes reported in Britain and Svalbard, in terms of morphology and internal architecture. Apparent stacking of slabs of subglacially-derived sediments (S2), such as documented in Britain and Svalbard by Hambrey et al. (1997), have also been imaged in some mounds on Lake Ladoga (Fig. 4a). Few mounds also display rectilinear slopes facing up-glacier, and irregular, down-glacier facies as their terrestrial counterparts in Britain and Svalbard, which is particularly well observed for the SE-mound in Fig. 4a.

Thrusting of subglacial material as a potential mechanism to explain the formation of the Ladoga mounds is also supported by the presence of apparent ramps, as the one inferred in the NW-mound on line 20 (Fig. 4a, to the right). The presence of folded structures, such as near the base of the SE-mound in Fig. 4a (to the left), further indicates that bulldozing and squeezing up of pre-existing S2-sediments over Sb1 contributed in forming the mounds (Fig. 4c-d). Sb1 may have, hence, acted as a décollement surface in several places. As each mound is bounded at its top by Sb2, which marks the retreat of the SIS in the Ladoga basin, we interpret the Ladoga mounds as an assemblage of individual ice-marginal landforms resulting from the decay of the active SIS after the LGM (Fig. 8b and c). Thus, we regard the well-preserved, ~90-m-thick sedimentary succession in the southern region (Figs. 3c and 4c,d) as a remnant of the initial stratigraphy of the sequence S2 which would have been preserved from the geological processes that formed the moraine mounds.

### 5.1.3. Paleovalleys and cut-and-fill channels

A complex history of erosion and infilling of a few paleovalleys has been captured near the southern and western shorelines (Figs. 3b, S1). These paleovalleys highly resemble glacial valleys imaged in the North and Baltic Sea (e.g. Huuse and Lykke-Andersen, 2000; Al Hseinat and Hübscher, 2014), and are, hence, regarded as such. These paleovalleys seem to be absent next to the moraine mounds whilst a dense network has been captured in the southern region, where merely a few mounds have been documented (Fig. 3b). The absence of valleys nearby mounds or in other areas may also result from a partial coverage of the MCS data. Glacial valleys are usually filled by discharged meltwater-sediments, supplied when the ice mass receded (Fig. 8c). Different aggradational stages in the paleovalleys development have been observed as well as vertical alignment of V-shaped indentations, which suggest no lateral change in the sediment-flow pathways over time (Fig. 3b). As Sb2 caps most of the paleovalleys, we relate them to the LGM glaciation and formed during the SIS retreat.

Nonetheless, the largest paleovalley documented near the western shoreline and illustrated in Fig. S1 displays a well-bedded facies onlapping its WSW hanging wall that could represent S2-remnant stratigraphy (*Facies a*). This would suggest an older age of formation for this paleovalley; possibly of MIS6-age (Saalian/Moscow glaciation). Yet, the paleovalleys reported in Lake Ladoga are predominantly of LGM-age; further coring data would, hence, be required to better constrain the age of the paleovalley (Fig. S1).

The numerous, transparent and often stacked, V-shaped features observed in S2 and S3 (Figs. 5a, b, d and S2d), are interpreted as cut-and-fill channels resulting from releases of meltwater discharges of the SIS as it decays. Interestingly, these features disappear along a stratigraphic surface that we refer to as 'H' within the varved sequence S3 (Figs. 2b and 5b).

### 5.1.4. Debris flows and mass-transport deposits

A multitude of thin, transparent layers has been observed in the echo-sounder data covering, in places, the cut-and-fill channels identified in the lower section of S3 (Fig. 5b) or draping the base of S4 (Figs. 4b and 5a/c, 6a, 7a). The association of the transparent layers in S3 with the cut-and-fill channels, along with their strong resemblance with debris-flow deposits captured in similar settings (Emmer, 2017), leads us to interpret the S3-layers as former debris flows induced from glacial meltwater discharges. The prominent reflections separating them are then regarded as marking different meltwater pulses over short timescales (Fig. 5b).

The transparent layer at the base of S4 displays variable thicknesses within the lake basin. The S4-layer is often thicker near the shorelines, which suggests that it likely originates from different

source areas. On the basis of its acoustic signature and similarities with other lacustrine settings, the S4-layer could either result from debris flows or turbidity currents (e.g. Zaremba and Scholz, 2019). Yet, its location at the same stratigraphical level indicates a contemporaneous time of emplacement regardless of its origin.

Massive transparent deposits have also been imaged within S3 in the southern, central and northern parts of the lake basin, which strongly contrasts with the finely-layered and undisturbed character of the varved sediments (Figs. 4b and 5c,d). Near the northern shoreline, the deposits eroded the underlying varves (Fig. 5c). In contrast, near the western shoreline, the bodies conformably draping the varved succession show a non-erosive behavior during their emplacement (Fig. 5d). These transparent deposits bear similarities with reflection-free deposits documented in the Oneida Lake basin, New York; interpreted by Zaremba and Scholz (2019) either as distally sourced turbidites triggered by seismic activity during glacio-isostatic rebound, or as the products of deglacial meltwater pulses from the ice front. On the basis of their acoustic signature (i.e. transparent facies, smooth and flat upper surface), we consider these transparent deposits as former, more massive, debris flows.

Other transparent deposits have also been highlighted at the base of S4 in the northernmost part of Lake Ladoga (Fig. 6b). These deposits, which tend to accumulate on top of each other, are usually separated by thin, reflective horizons. This indicates a relatively close time of emplacement. Interestingly, these deposits are located at the foot of the normal faults identified in the MCS data (Fig. 6b). We interpret these transparent bodies as mass-transport deposits (MTDs) resulting from the faults activity. Few MTDs have also been noted at the foot of some S2-mounds (Fig. 4b). We consider these MTDs as resulting from collapses of the moraine mounds as the SIS retreats.

## 5.2. Depositional history of Lake Ladoga

### 5.2.1. Pre-LGM (131 ka BP – ~20 ka BP)

The pre-LGM history of northwestern Russia, and particularly its Early Weichselian history, is fragmentarily known due to the widespread erosion of the SIS during the LGM. Marine interglacial clays retrieved at Lake Ladoga in 1934, from ~40-m-long drilled cores in the southwestern region (Fig. 1), showed rich content of marine diatom flora of Eemian age (MIS 5e; known in Russia as Mikulino). These sediments were, then, regarded as deposited during a time when Lake Ladoga was part of a marine seaway that was connecting the Pre-Baltic Sea to the Pre-White Sea (Cheremisinova, 1957). The palynological study carried out on the ~10-m-thick, basal sediments of core Co1309 (e.g. Andreev et al., 2019, Fig. 1) comforted the presence of Eemian sediments in Lake Ladoga, which are represented in the MCS data by the uppermost section of the sequence S2 at the coring site location (Figs. 2a and 8a). New insights into the vegetation and climate history during the late Eemian/Early Weichselian were, hence, provided by Andreev et al. (2019). The paleoenvironmental and paleoclimatic conditions derived from investigating these Co1309-sediments underlined a period significantly warmer at the end of the Eemian (MIS 5e), and possibly at the beginning of the Early Weichselian (early MIS 5d), compared to the Holocene, which is in agreement with terrestrial observations near St. Petersburg, along the Gulf of Finland and around Lake Ladoga (e.g. Abakumenko et al., 1977; Saltykova & Travina, 1977; Malakhovskii et al., 2000; Raukas, 1991; Krasnov et al., 1995; Funder et al., 2002; Miettinen et al., 2002, 2014 and references therein). According to Funder et al. (2002), Lake Ladoga was solely connected to the Pre-Baltic and the Pre-White Sea through the Karelian Seaway at the beginning of the Eemian interglacial, and as early as c. 130 ka according to

Miettinen et al. (2014). A progressive closure of this connection would have occurred after the end of the marine highstand, at c. 124 ka (Miettinen et al., 2014). The presence of freshwater green algae remains, cysts of marine and brackish-water dinoflagellates and acritarchs in the preglacial sediments findings led Andreev et al. (2019) led to conclude that Lake Ladoga was a bay of the Pre-Baltic Sea until, at least, c. 80 ka BP.

### 5.2.2. LGM (~20 ka BP – 13.9 ka cal. BP)

Following the Eemian (Mikulino) interglacial, the SIS inundated the region and eroded Quaternary sediments that accumulated in the lacustrine basin before. Overriding of the SIS is reflected in Lake Ladoga by the presence of a hiatus of ~60 ka in core Co1309 (e.g. Andreev et al., 2019; Gromig et al., 2019) along with an erosional unconformity (Sb2) in the MCS data (Figs. 3a, 4c and 6a). The moraine mound complexes underline subglacial thrusting and bulldozing processes of pre-existing sediments according to Co1309 findings. The variable degree of preservation of the moraine mounds and their variations in morphology, size and internal architecture suggest oscillations during the recession (Fig. 8b and c). The large sub-conical and uneven mounds with their relatively well-preserved internal architecture (Fig. 4a; between offsets 64,700–67,600), likely reflect a single-phase build up during the retreat. In contrast, the sub-rounded to lens-shaped mounds with an overall smooth morphology and complex internal architecture (NW mound in Fig. 4a) may reflect subsequent motion of the SIS during periods of minor re-advances and would explain the intense degree of deformation captured in these mounds. These oscillations are also reflected by the prominent internal reflections near the base of several mounds (Fig. 4a) marking short-lived, overriding phases.

The morphology and distribution pattern of the moraine mounds may also reflect a complex pattern and shape of the paleo-ice front, as reported in other glaciated settings. Such a random mounds distribution may denote variations either in the substrate (sediments more or less easily eroded, thrusted, bulldozed) or in the ice-flow dynamics (more or less erosive). The remnant stratigraphy of S2-sediments in the southern region (Figs. 3c and 4d) favours the second hypothesis and suggests that the SIS was less erosive to the south than in the centre and to the north, where the mounds have been mostly documented. This difference in erosion may be the result of a thinning of the SIS in the southern region. Elsewhere, the SIS would have been thick enough to vigorously bulldoze, subglacially thrust and erode pre-existing sediments, hence, form the mounds. Thinning out of the SIS to the south at the time when the mounds formed elsewhere is also supported by the presence of several paleo-glacial valleys and dense cut-and-fill channels (Figs. 3b and 5a, c, d), which suggests rather intense meltwater discharges. The progressive erosion towards the central lake basin is denoted on two specific profiles, where the upper S2-seismic Facies b is being eroded first (Fig. 3c), followed by the lower Facies a (Fig. 4d). Beyond this area, the moraine-mound complex field spreads out.

### 5.2.3. Deglaciation (13.9–11.4 ka cal. BP)

Following the ice recession, Lake Ladoga became part of the BIL and varved sediments accumulated in the lacustrine basin from ~13.9 cal ka BP at site Co1309 (Gromig et al., 2019, Fig. 8d). Assuming an ice retreat of  $\sim 110 \pm 2 \text{ m a}^{-1}$  and a constant or slightly decreasing sedimentation rate throughout deposition of LZ IV ( $\sim 4.4 \text{ mm a}^{-1}$ ; Gromig et al., 2019), we infer an onset of the varve sedimentation in the southern lake basin earliest around ~14.3 ka.

During the initial ice retreat, from 13.9 to 13.2 cal ka BP (e.g. Gromig et al., 2019), significant meltwater discharges eroded the lower section of S3 and led to numerous cut-and-fill channels and

massive transparent deposits (Fig. 5d). Several pulses of meltwater discharges by debris flows occurred during that time in many places (Fig. 5b). The cut-and-fill channels and debris flows disappear in the MCS data along a stratigraphic surface 'H' (Figs. 2b and 5b) that is overlaid by well-bedded and undisturbed reflections. We, thus, regard this surface 'H' as marking the last time when the SIS had a very proximal position to Lake Ladoga that allowed erosion and subsequent filling of the cut-and-fill channels into already-deposited varved sediments. Tracing back 'H' to coring site Co1309 (Fig. 2b), and assuming a sedimentation rate of  $\sim 4.4 \text{ mm a}^{-1}$  in LZ IV (=S3), we tentatively date 'H' at  $\sim 13.4 \text{ cal ka BP}$ ; which precedes the end of the initial ice retreat by  $\sim 200$  years (e.g. Gromig et al., 2019).

During the final ice retreat, from 12.3 to 11.4 cal ka BP (e.g. Gromig et al., 2019), massive transparent deposits eroding (Fig. 5c), or conformably draping the varves (Fig. 5d), accumulated to the north. The stratigraphy of these deposits suggests an emplacement at the end of the varve sedimentation; most likely during the third stage of the final ice retreat, at the onset of the Holocene (11.6–11.4 cal ka BP; e.g. Gromig et al., 2019). The BIL drainage c.  $11,620 \pm 100 \text{ cal a BP}$  (Stroeven et al., 2015) resulted in a catastrophic flood event that caused a 25-m-lowering of water level at Lake Ladoga (Björck, 1995; Jakobsson et al., 2007; Subetto, 2009; Bennike and Jensen, 2013; Stroeven et al., 2015). This age coincides with the age inferred for these massive deposits. Together with the conclusions drawn at Lake Oneida (e.g. Zaremba and Scholz, 2019), we suggest that the non-erosive deposits identified near the northwestern shoreline (Fig. 5d) may be related to the BIL drainage. Overlying S3-sediments support this interpretation, as they likely correspond to varves that accumulated over the next  $\sim 200$  years, i.e., until 11.4 cal ka BP, when the SIS retreated from the Ladoga catchment area.

In contrast, the massive deposits that eroded S3 are directly overlain by a highly-reflective horizon likely made of coarse-grained material (Fig. 5c). The absence of varves draping these deposits suggests a later timing of emplacement, closer to 11.4 cal ka BP. This age coincides with a short-lived stagnation phase of the SIS, called "11.4 ka event", which formed the Salpausselkä III Moraine further to the northeast during the Preboreal Oscillation (PBO) (Fig. 1a; Rasmussen et al., 2014; Stroeven et al., 2016). Fisher et al. (2002) attributed the PBO to a massive meltwater discharge from an abrupt drainage of glacial Lake Agassiz, Canada. It is, hence, possible to assume that, similarly to its counterpart in Canada, these erosive deposits might result from meltwater discharges of the SIS during a temporary halt throughout the overall retreat. This halt was dated at c. 11.45 cal ka BP at site Co1309 (e.g. Gromig et al., 2019), which concurs well with the PBO short-lived stagnation phase reported in the region (e.g. Rasmussen et al., 2014).

#### 5.2.4. Holocene (11.4 ka cal. BP – present)

The termination of the varve sedimentation (S3) marks the retreat of the SIS beyond the catchment of Lake Ladoga and the onset of normal lacustrine sedimentation (S4) (Fig. 8e). The age-depth model derived at Site Co1309 indicates an age of  $11.38 \pm 0.14 \text{ cal ka BP}$  for this transition (Gromig et al., 2019), which slightly post-dates the onset of the Holocene dated at  $11.65 \pm 0.1 \text{ cal ka BP}$  (Rasmussen et al., 2014). The sequence S4, hence, post-dates the drainage of the BIL and the formation of the Salpausselkä II moraine north of Lake Ladoga (Fig. 1a) according to recent dating.

Lake Ladoga experienced several shoreline displacements since the retreat of the SIS. Following the BIL drainage at 11.62 cal ka BP (Stroeven et al., 2015) and significant lake-level lowering of  $\sim 25 \text{ m}$  (e.g. Saarnisto, 2012), the varved succession (S3) has been strongly eroded over a widespread area and an acoustically strong reflection truncates the upper section near the shorelines (Fig. 7). This highly-

reflective horizon likely corresponds to the sandy unit documented on top of varves in small lakes situated NW of Lake Ladoga and in the Karelian Isthmus, and interpreted as a hiatus (Subetto, 2009). From its location in the sequence stratigraphy, together with its widespread extent, we interpret this erosional surface as a stratigraphic marker of the Ladoga lake-water level after the BIL drainage. In places, this erosional surface conformably drapes the varves basinwards (Fig. 7a) and we interpret this draping as a result of coarse-grained material accumulation in very shallow waters near the post-BIL drainage shorelines. This water-level drop caused most of the moraine mounds to reach the surface, leading to erosion and reshaping of their upper section (Figs. 7b and 8e). In the southern and eastern regions, the prominent reflection surfacing the mounds is much thicker and reflective than elsewhere. This likely reflects the contribution of subsequent erosions in surfacing and reshaping the mounds (Fig. 7b), which also likely further eroded S3.

The ongoing and regional post-glacial isostatic uplift led to intense tectonic activity in the northern lake basin and triggered accumulations of several MTDs in a short time period during the early Holocene (Fig. 6b). This isostatic uplift also led to considerable changes in the hydrological system of Lake Ladoga. During the so-called Ladoga Transgression (5–3 cal ka BP; Dolukhanov et al., 2009), the lake-level rose by  $\sim 10 \text{ m}$  (i.e.  $>20 \text{ m a.s.l.}$ ; Saarnisto and Grönlund, 1996). The multi-reason, long-lasting Ladoga Transgression (c. 2000–2500 years) is reflected in the echounder data by the character and distribution of the sequence S4 (Figs. 2b, 5, 6b and 7). The erosional truncation noted in the uppermost section of S4, occurring close to and along the eastern and southern shorelines, likely reflect the lowering of the lake level associated to the formation of the Neva River to the south (modern outlet; Fig. 1b) at  $\sim 3.35 \text{ cal ka BP}$  (Malachovskii et al., 1996; Dolukhanov et al., 2009, 2010; Saarnisto and Grönlund, 1996; Saarnisto, 2012). The continuity of this truncation within the sedimentary sequence most likely reflects shallow water areas, where fine-grained sediments became winnowed and coarse-grained sediments accumulated. In the southernmost and eastern regions, more particularly, the formation of the Neva River led to a strong erosion of the underlying sequence S3 (Fig. 7b). Surficial and local erosional surfaces have been noted along the northern, eastern and western shorelines, which might reflect recent seasonal lake-level fluctuations (Fig. 6b).

#### 5.3. Regional implications

The new data contributed considerably to further understanding the behavior of the SIS in NW Russia during the LGM by providing new key observations to Stroeven et al. (2016) and Hughes et al. (2016) reconstructions. Analysis of the MCS data reveals unreported, buried to outcropping, glacial landforms (i.e. moraine mounds, glacial paleovalleys, cut-and-fills channels, debris flows) that further constrains the ice sheet behavior during its retreat, which was only fragmentarily known in this region.

According to Hughes et al. (2016)'s time-slice reconstructions of the SIS extent during the last 40 ka, the northernmost part of Lake Ladoga would have been covered by ice as early as 25 ka. In their most-credible scenario, however, the SIS would have reached Lake Ladoga thousand years later, at 24 ka, covering about  $\frac{2}{3}$  of its surface area, and would have covered the entire lake basin from 23 ka to 14 ka. According to data from sediment core Co1309 (e.g. Gromig et al., 2019), the onset of the SIS deglaciation in the northwesternmost part of the lake was at 13.9 cal ka BP. This would also imply an earlier start of the SIS decay in the southern lake region that we tentatively dated sometime between 15.9 and 14.5 cal ka BP. The coring results rather support the minimum

extent proposed by [Hughes et al. \(2016\)](#) as the SIS' most-credible extent at 14 ka, and also reconsider the SIS extent depicted by Stroeven et al. (2016) for the same period of time. However, our observations concur with the SIS extent portrayed by the authors at 13 ka, in the Ladoga region.

Ice-margin oscillations have been recognized on land for the SIS during its recession in NW Russia, Sweden and Norway ([Hughes et al., 2016](#); [Stroeven et al., 2016](#)). However, the time-slice reconstructions from [Hughes et al. \(2016\)](#) and [Stroeven et al. \(2016\)](#) did not attempt to picture re-advance positions of the SIS at smaller time scales (i.e. <1000 years). Investigation of the MCS data from the PLOT project documents, for the first time, a series of moraine mounds which displays variable degrees of preservation and internal deformation that attests for subsequent motion of the SIS in the Ladoga region during periods of minor re-advances following the LGM. The seismic signature of the moraine mounds also informs on the mechanisms at their origin (subglacial thrusting of pre-existing sediments and bulldozing), hence, providing new key constraints on the SIS behavior in NW Russia necessary to acquire/have to model and understand its past dynamics. The morphology and distribution pattern of the mounds reflect a complex pattern and shape of the SIS paleo-ice front as already visible on the reconstructions in NW Russia, at different time periods. This random distribution, together with the preservation of remnant stratigraphy of S2-sediments that compose the mounds, also denotes variations in the ice-flow dynamics and underlines a character less erosive for the SIS in the southern region than in the central and northern ones, where the SIS was vigorous enough to bulldoze, subglacially thrust and erode S2-sediments to form the mounds. The discovery of paleo-glacial valleys and cut-and-fill channels attests for intense meltwater discharges during the decay of the SIS and also support a thinning of the ice sheet in the southern region at the time where the mounds are buildup elsewhere. A detailed characterization of the SIS episodic retreat in the Ladoga basin, to be compared and placed in the regional evolution of the SIS growth and decay models such as depicted by [Hughes et al. \(2016\)](#) and [Stroeven et al. \(2016\)](#), would require acquisition of a denser network of coring/drilling and geophysical data sets.

## 6. Conclusions

The MCS and echo-sounder data gathered on Lake Ladoga provided a unique opportunity to image its sedimentary infill in unprecedented detail, thus, enhancing our current understanding on the origin, development and evolution of lacustrine basins in formerly glaciated areas. The high resolution and dense grid coverage of the acoustic data collected in the framework of the PLOT project, in conjunction with sedimentological information available, provided new insights into the stratigraphy and structure of the lacustrine basin as summarized below.

- The new data allowed us to establish a complete and robust reconstruction of Lake Ladoga's pre- and post-glacial (i.e. LGM) depositional and environmental history, including past ice coverage, lake-level fluctuations and tectonic activities.
- Kilometre-scale, sublacustrine landforms interpreted as moraine-mound complexes formed during the overall retreat of the Scandinavian Ice Sheet (SIS) after the LGM (Late Valdai; MIS 2) and would result from bulldozing and subglacial thrusting of pre-existing lacustrine sediments (S2). The variable degree of preservation of the Ladoga mounds suggests oscillations of the SIS during its overall recession, whilst preserved remnant stratigraphy to the south indicates a less erosive character of the SIS; therefore, a progressive retreat.

- As a result of the deglaciation, varved sediments accumulated in the basin (S3). A dense network of paleovalleys and cut-and-fill channels witnessed intense and sudden releases of meltwater discharges related to SIS decay and retreat from Ladoga's basin.
- Massive transparent deposits likely document the drainage of the BIL into the North Sea, while the significant lake-level lowering is marked in the basin by a highly reflective horizon.
- Erosional truncation in the recent lacustrine sedimentary succession (S4) marked the formation of the Neva River (modern lake outlet) and, consequently, the end of the Ladoga Transgression (~3.35 cal ka BP).

These observations provided new information regarding the location, dynamics and behavior of the SIS in the Ladoga region during the overall retreat, thus providing important constraints for numerical models assessing ice-sheet responses to past climate. The sedimentary succession at Lake Ladoga provides a new stratigraphic framework for future investigations in the region. Our study also contributes to refine seismic facies models for similar lakes, independently of their locations, which helps improving our overall understanding of past-ice sheet dynamics and behavior, and paleoenvironmental changes in the NW Russian region during the last Quaternary glaciations. Finally, our results emphasizes on the importance of integrating geophysical and sedimentological data to reconstruct a most complete and detailed preglacial and postglacial depositional, environmental and climatic history of formerly-glaciated lacustrine basins.

## Declaration of competing interest

The authors declare that they have no known competing financial interests or personal relationships that could have appeared to influence the work reported in this paper.

## Acknowledgments

We thank the captain, officers, crews and scientific team aboard the R/V Poseidon for their efficient work on Lake Ladoga during the acquisition of the seismic data. Financial support for this study was provided by the German Federal Ministry for Education and Research (BMBF; Grants 03G0839B, Grant 03G0859A, Grant 03F0830B). The work of G. Fedorov was partly funded by the Russian Foundation for Basic Research (project No. 18-05-60291). D. Subetto received support from the Russian Science Foundation (project No. 18-17-00176) and from the Ministry of Science and Higher Education of the Russian Federation (project No. FSZN-2020-0016). The IHS Kingdom® and Schlumberger Vista® software provided free academic licenses at Kiel University. The authors thank Shrey Badhani for fruitful comments on an earlier version of the manuscript. We are also grateful to the Editor, Colm O'Cofaigh, and two anonymous reviewers for their constructive suggestions, which strengthened the study and improved the manuscript.

## Appendix A. Supplementary data

Supplementary data to this article can be found online at <https://doi.org/10.1016/j.quascirev.2020.106637>.

## Authors contribution

E. Lebas wrote the manuscript, created the figures, processed and interpreted the seismic data. T. Averes and C. Götz helped processing the seismic data for multiple removal. B. Wagner processed the echosounder data. R. Gromig provided information regarding core Co1309. D. Subetto and G. Fedorov provided relevant

literature only available in Russian language and helped with the translation. M. Naumenko created the shaded relief map of Lake Ladoga shown in Fig. 1c. S. Krastel and M. Melles led the seismic and the coring campaigns, respectively. All co-authors took part in the scientific discussion and reviewed the manuscript.

## References

- Abakumenko, G.S., Ladyshkina, T.E., Saltykova, V.F., Semicheva, V.I., Usikova, T.V., 1977. Marine interglacial deposits on the northern part of Karelian Isthmus. In: Biske, G.S. (Ed.), *Stratigrafiya I Paleogeografiya Chetvertichnogo Perioda Severa Evropeiskoi Chasti SSSR*. Institute of Geology, Karelian Branch of Academy of Science SSSR, Petrozavodsk, pp. 93–97 (in Russian).
- Ailio, J., 1915. Die geographische Entwicklung des Ladogasees. *Fennia* 8 (3), 157 s.
- Al Hseinat, M., Hübscher, C., 2014. Ice-load induced tectonics controlled tunnel valley evolution – instances from the southwestern Baltic Sea. *Quat. Sci. Rev.* 97, 121–135.
- Alekin, O.A., Smirnova, A.P., 1984. Natural Resources of Large Lakes and Their Future Changes. Nauka, Leningrad, p. 286 (In Russian).
- Aleksandrovskii, A.L., Arslanov, Kh. A., Davydova, N.N., Dolukhanov, P.M., Zaitseva, G.I., Kirpicnikov, A.N., Kuznetsov, D.D., Lavento, M., Ludikova, A.V., Nosov, E.N., Savel'eva, L.A., Sapelko, T.V., Subetto, D.A., 2009. New data on the Ladoga transgression, the Neva River formation, and agricultural development of northwestern Russia. *Dokl. Earth Sci.* 425 (2), 274–278.
- Amantov, A.V., 2014. Geology of pre-Quaternary deposits and tectonic of Lake Ladoga. *Regional Geology and Metallogenesis* 58, 22–32 (In Russian).
- Amantov, A.V., Amantova, M.G., 2014. Development of Lake Ladoga's depression from standpoint of glacial theory. *Regional Geology and Metallogenesis* 59, 5–14 (In Russian).
- Andreev, A.A., Shumilovskikh, L.S., Savelieva, L.A., Gromig, R., Fedorov, G.B., Ludikova, A., Wagner, B., Wennrich, V., Brill, D., Melles, M., 2019. Environmental conditions in northwestern Russia during MIS5 inferred from the pollen stratigraphy in a sediment core from Lake Ladoga. *Boreas* 48, 377–386.
- Andrén, T., Lindeberg, G., Andrén, E., 2002. Evidence of the final drainage of the baltic Ice Lake and the brackish phase of the Yoldia Sea in glacial varves from the Baltic Sea. *Boreas* 31, 226–238.
- Andrén, T., Barker Jørgensen, B., Cotterill, C., Green, S., the IODP expedition scientific party, 2015. IODP expedition 347: Baltic Sea basin paleoenvironment and biosphere. *Sci. Drill.* 20, 1–12.
- Anokhin, V., Naumenko, M., Subetto, D., Nesterov, N., 2018. Geomorphological features of the bottom of lake Ladoga. *Geophys. Res. Abstr.* 20. EGU2018-1795, Vienna.
- Bakhmutov, V.G., Zagniy, G.F., 1990. Secular variation of the geomagnetic field: data from the varved clays of Soviet Karelia. *Phys. Earth Planet. In.* 63, 121–134.
- Bakhmutov, V.G., Davydova, N.N., Delyusina, I.V., Rybalko, A.E., Subetto, D.A., 1993. Late- and postglacial development history of Lehmalhti Bay. In: Davydova, N.N., Koshechkin, B.I. (Eds.), *Evolyutsiya Okruzhaeshei Sredy I Sovremennoi Status Geosistemy Ladozhskogo Ozera* (The Evolution of Natural Environments and Current State of the Lake Ladoga Geosystem). Russian Geographical Society, St. Petersburg, pp. 34–43 (In Russian).
- Batchelor, C.L., Dowdeswell, J.A., 2016. Lateral shear-moraines and lateral marginal-moraines of palaeo-ice streams. *Quat. Sci. Rev.* 151, 1–26.
- Batchelor, C.L., Dowdeswell, J.A., Rignot, E., 2018. Submarine landforms reveal varying rates and styles of deglaciation in North-West Greenland fjords. *Mar. Geol.* 402, 60–80.
- Bennike, O., Jensen, J.B., 2013. A baltic Ice Lake lowstand of latest allerød age in the arkona basin, southern Baltic Sea. *Geol. Surv. Den. Greenl. Bull.* 28, 17–20.
- Beres, M., Gilli, A., Ariztegui, D., Anselmetti, F.S., 2008. The Lago Cardiel Basin, Argentina (49°S): origin and evolution revealed by high-resolution multi-channel seismic reflection studies. *J. S. Am. Earth Sci.* 25, 74–85.
- Björck, S., 1995. A review of the history of the Baltic Sea, 13.0–8.0 ka BP. *Quat. Int.* 27, 19–40.
- Charlet, F., De Batist, M., Chapron, E., Bertrand, S., Pino, M., Urrutia, R., 2008. Seismic stratigraphy of lago puyehue (Chilean lake district): new views on its deglacial and Holocene evolution. *J. Paleolimnol.* 39, 163–177.
- Cheremisinova, E.A., 1957. Marine diatom flora of Quaternary sediments from Ladoga basin. *Byulluten Komissii po Izucheniyu Chetvertichnykh Otlozhennii* 21, 105–112 (in Russian).
- Davydova, N.N., 1985. Diatoms as Indicators of Ecological Conditions in Water Basins in Holocene. Nauka, Leningrad, p. 244 (In Russian).
- Davydova, N.N., 1990. Change of ecological conditions in Lake Ladoga according to diatom analysis data. In: Kvasov, D.D., Martinson, G.G., Raukas, A.V. (Eds.), *History of Lakes Ladoga, Onega, Pskovsko-Chudskoye, Baikal and Khanka*. Nauka, Leningrad, pp. 53–62 (In Russian).
- Davydova, N.N., Rybalko, A.E., Subetto, D.A., Khomutova, V.I., 1998. The late pleistocene history of lake Ladoga. In: Khomutova, V.I., Davydova, N.N., Raukas, A.V., Rumyantsev, V.A. (Eds.), *The Pleistocene Lake History of the East European Plain*. Nauka, St. Petersburg, pp. 134–140 (In Russian).
- Dolukhanov, P.M., 1979. The quaternary history of the baltic. Leningrad and soviet carelia. In: Gudelis, V., K Unigsson, L.-K. (Eds.), *The Quaternary History of the Baltic*. Acta Univ. Upsaliensis Symp. Univ. Upsaliensis Annum Quingentesimum Celebrantis, vol. 1, pp. 115–125.
- Dolukhanov, P.M., Subetto, D.A., Arslanov, K., Davydova, N.N., Zaitseva, G.I., Djinoridze, E.N., Kuznetsov, D.D., Ludikova, A.V., Sapelko, T.V., Savelieva, L.A., 2009. The Baltic Sea and Ladoga lake transgressions and early human migrations in north-western Russia. *Quat. Int.* 203, 33–51.
- Dolukhanov, P.M., Subetto, D.A., Arslanov, Kh. A., Davydova, N.N., Zaitseva, G.I., Kuznetsov, D.D., Ludikova, A.V., Sapelko, T.V., Savelieva, L.A., 2010. Holocene oscillations of the Baltic Sea and Lake Ladoga levels and early human movements. *Quat. Int.* 220, 102–111.
- Donner, J., Raukas, A., 1992. Late- and postglacial development of the Gulf of Finland. 2. Baltic Ice Lake. In: Raukas, A., Hyvarinen, H. (Eds.), *Geology of the Gulf of Finland*, Estonian Academy of Sciences. Academy of of Finland, pp. 262–276.
- Dowdeswell, J.A., Evans, J., Cofaigh, C.O., 2010. Submarine landforms and shallow acoustic stratigraphy of a 400 km-long fjord-shelf-slope transect, Kangerlussuaq margin, East Greenland. *Quat. Sci. Rev.* 29, 3359–3369.
- Emmer, A., 2017. Glacier retreat and glacial Lake outburst floods (GLOFs). In: Cutter, L.S. (Ed.), *Oxford Research Encyclopaedia - Natural Hazard Science*. Oxford University Press, New York, pp. 1–38.
- Fisher, T.G., Smith, D.G., Andrews, J.T., 2002. Prebreval oscillation caused by a glacial Lake Agassiz flood. *Quat. Sci. Rev.* 21, 873–878.
- Funder, S., Demidov, I., Yelovicheva, Y., 2002. Hydrography and mollusc faunas of the baltic and the White sea-North Sea seaway in the eemian. *Palaeogeogr. Palaeoclimatol. Palaeoecol.* 184, 275–304.
- Gorlach, A., Hang, T., Kalm, V., 2017. GIS-based reconstruction of Late Weichselian proglacial lakes in northwestern Russia and Belarus. *Boreas* 46, 486–502.
- Graham, D.J., Midgley, N.G., 2000. Moraine-mound Formation by Englacial Thrusting: the Younger Dryas Moraines of Cwm Idwal, North Wales, vol. 176. Geological Society, London, Special Publications, pp. 321–336.
- Greenwood, S.L., O'Regan, M., Swärd, H., Flodén, T., Ananyev, R., Chernykh, D., Jakobsson, M., 2015. Multiple re-advances of a Lake Vättern outlet glacier during Fennoscandian Ice Sheet retreat, southcentral Sweden. *Boreas* 44, 619–637.
- Gromig, R., Wagner, B., Wennrich, V., Fedorov, G., Savelieva, L., Lebas, E., Krastel, S., Brill, D., Andreev, A., Subetto, D., Melles, M., 2019. Deglaciation history of Lake Ladoga (northwestern Russia) based on varved sediments. *Boreas* 48, 330–348. <https://doi.org/10.1111/bor.12379>. ISSN 0300-9483.
- Hambrey, M.J., Huddart, D., 1995. Englacial and proglacial glaciectonic processes at the snout of a thermally complex glacier in Svalbard. *J. Quat. Sci.* 10, 313–326.
- Hambrey, M.J., Huddart, D., Bennett, M.R., Glasser, N.F., 1997. Genesis of 'hummocky moraines' by thrusting in glacier ice: evidence from Svalbard and Britain. *J. Geol. Soc.* 1997 (154), 623–632.
- Hang, T., Gurbich, V., Subetto, D., Strakhovenko, V., Potakhin, M., Belkina, N., Zobkov, M.A., 2019. Local clay-varve chronology of Onega Ice Lake, NW Russia. *Quat. Int.* 524, 13–23.
- Hughes, A.L.C., Gyllencreutz, R., Lohne, Ø.S., Mangerud, J., Svendsen, J.I., 2016. The last Eurasian ice sheets – a chronological database and time-slice reconstruction, DATED-1. *Boreas* 45, 1–45.
- Huuse, M., Lykke-Andersen, H., 2000. Quaternary valleys in the eastern Danish North Sea: morphology and origin. *Quat. Sci. Rev.* 19 (12), 1233–1253.
- Jakobsson, M., Björck, S., Alm, G., Andrén, T., Lindeberg, G., Svensson, N.-O., 2007. Reconstructing the younger Dryas ice dammed lake in the Baltic basin: bathymetry, area and volume. *Global Planet. Change* 57, 355–370.
- Johnson, T.C., Werne, J.P., Brown, E.T., Abbott, A., Berke, M., Steinman, B.A., Halbur, J., Contreras, S., Grosshuesch, S., Deino, A., Scholz, C.A., Lyons, R.P., Schouten, S., Damsté, J.S., 2016. A progressively wetter climate in southern East Africa over the past 1.3 million years. *Nature* 537, 220–224.
- Kalm, V., 2012. Ice-flow pattern and extent of the last scandinavian ice sheet southeast of the Baltic Sea. *Quat. Sci. Rev.* 44, 51–59.
- Kostrova, S.S., Meyer, H., Bailey, H.L., Ludikova, A.V., Gromig, R., Kuhn, G., Shibaev, Y.A., Kozachek, A.V., Ekyaykin, A.A., Chapligin, B., 2019. Holocene hydrological variability of Lake Ladoga, northwest Russia, as inferred from diatom oxygen isotopes. *Boreas* 48, 361–376.
- Krasnov, I.I., Reineke, V.I., 1936. About gas-bearing capacity of the Leningrad region Quaternary deposits. In: Golubyatnikov, V.D., Khlopkin, V.G. (Eds.), *Prirodnye Gazy. Sbornik* 11, 3–31. Glavnaya Redakziya Geologo-Razvedochnoi I Geodezicheskoi Literatury, Leningrad-Moscow (in Russian).
- Krasnov, I.I., Arslanov, K., Kazartseva, T.I., Tertychnaya, T.V., Chernov, S.B., Pleshivtseva, E.C., 1995. Key section of upper Pleistocene sediments of Neva lowland in Kelkolovo open pit. *Regional'naya Geol. Metallog.* 4, 88–99 (in Russian).
- Krastel, S., Leicher, N., Harms, U., 2017. Pre-site survey and drill site selection for lake sediment coring. In: Harms, U. (Ed.), *ICDPPrimer - Best Practices for Planning, Managing, and Executing Continental Scientific Drilling Projects*. International Continental Scientific Drilling Program, Potsdam, pp. 17–24.
- Kvasov, D., 1979. The Late-Quaternary history of large lakes and inland seas of Eastern Europe. *Annales Academiæ Scientiarum Fennicæ, Series A, III, Geol. Geogr.* 127, 71.
- Lebas, E., Krastel, S., Wagner, B., Gromig, R., Fedorov, G., Baumer, M., Kostromina, N., Haflidason, H., 2019. Seismic stratigraphical record of Lake Levinson-Lessing, Taymyr Peninsula: evidence for ice-sheet dynamics and lake-level fluctuations since the Early Weichselian. *Boreas* 48, 470–487. <https://doi.org/10.1111/bor.12381>. ISSN 0300-9483.
- Maksimov, A.V., Bogdanov, Yu. B., Voinova, O.A., Kossovaya, O.L., Bakhteev, A.R., Evdokimova, I.O., Gorbachevich, N.R., Nogina, M. Yu., Nikonova, A.S., Surikov, S.N., Chuyko, M.A., Shishlyannikov, A.N., Astafiev, B. Yu., Voinov, A.S.,

- Bogachev, V.A., Yanovskiy, A.S., Amontov, A.V., Androsov, E.A., Ivanova, N.O., Suslova, S.V., 2015. An explanatory note on a geological map of the Russian Federation of a scale of 1:1000000 (third generation). In: Baltic Series. Sheets P-(35), 36 (Petrozavodsk). VSEGEI Cartographic Factory, St. Petersburg, p. 400 ([In Russian]).
- Malakhovskii, D.B., Kotlukova, L.V., Spiridonov, M.A., 2000. Problems of stratigraphy and paleogeography of the Late Pleistocene of north-western Russia. Regional'naya Geol. Metallog. 12, 24–33 (in Russian).
- Malakhovsky, D.B., Markov, K.K. (Eds.), 1969. The Geomorphology and Quaternary Deposits of the Northwestern European USSR. Nauka, Leningrad, p. 256 ([In Russian]).
- Mandych, A.F., Shilkrot, G.S., 1995. Ladoga and Onega lakes. In: Mandych, A.F. (Ed.), Enclosed Seas and Large Lakes of Eastern Europe and Middle Asia, pp. 231–273.
- Markov, K.K., Poretzky, W.S., 1935. Pollen- and diatomeneanalytische Untersuchungen fiber die Geschichte des Finnischen Meerbusens, Ladoga- und Onegasées. Beih. Bot. Centralbl. 52 (B), 390–446.
- Melles, M., Brigham-Grette, J., Minyuk, P.S., Nowaczyk, N.R., Wennrich, V., DeConto, R.M., Anderson, P.M., Andreev, A.A., Coletti, A., Cook, T.L., Haltia-Hovi, E., Kukkonen, M., Lozhkin, A.V., Rosén, P., Tarasov, P., Vogel, H., Wagner, B., 2012. 2.8 Million years of Arctic climate change from Lake El'gygytgyn, NE Russia. Science 337, 315–320.
- Melles, M., Svendsen, J.I., Fedorov, G., Wagner, B., 2019. Northern Eurasian lakes – late Quaternary glaciation and climate history – introduction. Boreas 48, 269–272.
- Miettinen, A., Rinne, K., Haila, H., Hyvarinen, H., Eronen, M., Delusina, I., Kadastik, E., Kalm, V., Gibbard, P., 2002. The marine Eemian of the Baltic: new pollen and diatom data from Peski, Russia, and P-ohja-Uhtju, Estonia. J. Quat. Sci. 17, 445–458.
- Miettinen, A., Haila, H., Hyvärinen, H., Rinne, K., Eronen, M., 2005. Eemian crustal deformation in the eastern Baltic area in the light of the new sites at Peski, Russia and Pöhja-Uhtju, Estonia. Quat. Int. 130, 31–42.
- Miettinen, A., Head, M.J., Knudsen, K.L., 2014. Eemian sea-level high stand in the eastern Baltic Sea linked to long-duration White Sea connection. Quat. Sci. Rev. 86, 158–174.
- Mitchum, J.R.M., Vail, P.R., Sangree, J.B., 1977. Seismic stratigraphy and global changes of sea level, part 6: stratigraphic interpretation of seismic reflection patterns in depositional sequences. In: Payton, C.E. (Ed.), Seismic Stratigraphy Applications to Hydrocarbon Exploration, 117–133. American Association of Petroleum Geologists Memoir, p. 26.
- Malachovskii, D.B., Delusin, I.V., Gej, N.A., Dginoridzse, R.N., 1996. Evidence from the Neva River valley, Russia, of the Holocene history of lake Ladoga. Fennia 174, 113–123.
- Naumenko, M.A., 2013. Analysis of morphometric characteristics underwater relief of Lake Ladoga based on the digital model. Izvestiya Rossiiskoi Akademii Nauk. Seriya Geograficheskaya 1, 62–72 ([In Russian]).
- Naumenko, M.A., 2015. Three-dimensional image of bottom relief of Lake Ladoga. In: Rumyantsev, V.A. (Ed.), "Ladozhskoye Ozero i Yego Dostoprimechatel'nosti" (Atlas). SPb., Nestor-Istoriya, pp. 36–37.
- Ramsay, W., 1928. Eisgestaute Seen und Rezession des Inlandeises in Sudkarelien und Newatal. Fennia 50 (5), 21.
- Rasmussen, S.O., Bigler, M., Blockley, S.P., Blunier, T., Buchardt, S.I., Clausen, H.B., Cvijanovic, I., Dahl-Jensen, D., Johnsen, S.J., Fischer, H., Gkinis, V., Guillevic, M., Hoek, W.Z., Lowe, J.J., Pedro, J.B., Popp, T., Steierstad, I.K., Steffensen, J.P., Svensson, A.M., Vallelonga, P., Vinther, B.M., Walker, M.J.C., Wheatley, J.J., Winstrup, M., 2014. A stratigraphic framework for abrupt climatic changes during the Last Glacial period based on three synchronized Greenland ice-core records: refining and extending the INTIMATE event stratigraphy. Quat. Sci. Rev. 106, 14–28.
- Raukas, A., 1991. Eemian interglacial records in the northwestern European part of the Soviet Union. Quat. Int. 10–12, 183–189.
- Rinterknecht, V.R., Clark, P.U., Raisbeck, G.M., Yiou, F., Brook, E.J., Tschudi, S., Lunkka, J.P., 2004. Cosmogenic  $^{10}\text{Be}$  dating of the Salpausselkä 1 moraine in southwestern Finland. Quat. Sci. Rev. 23, 2283–2289.
- Reimer, P.J., Bard, E., Bayliss, A., Beck, J.W., Blackwell, P.G., Ramsey, C.B., Buck, C.E., Cheng, H., Edwards, R.L., Friedrich, M., Grootes, P.M., Guilderson, T.P., Haflidason, H., Hajdas, I., Hatté, C., Heaton, T.J., Hoffmann, D.L., Hogg, A.G., Hughen, K.A., Kaiser, K.F., Kromer, B., Manning, S.W., Niu, M., Reimer, R.W., Richards, D.A., Scott, E.M., Southon, J.R., Staff, R.A., Turney, C.S.M., van der Plicht, J., 2013. IntCal13 and Marine13 radiocarbon age calibration curves 0–50,000 years cal BP. Radiocarbon 55, 1869–1887.
- Rinterknecht, V.R., Clark, P.U., Raisbeck, G.M., Yiou, F., Bitinas, A., Brook, E.J., Marks, L., Zelcs, V., Lunkka, J.-P., Pavlovskaya, I.E., Piotrowski, J.A., Raukas, A., 2006. The last deglaciation of the southeastern sector of the Scandinavian Ice Sheet. Science 311, 1449–1452.
- Rumyantsev, V., Viljanen, M., Slepukhina, T., 1999. The present state of Lake Ladoga, Russia — a review. Boreal Environ. Res. 4, 201–214.
- Rumyantsev, V.A., Drabkova, V.G. (Eds.), 2002. Ladoga Lake: Past, Present, Future. Nauka, St. Petersburg, p. 327 ([In Russian]).
- Rybalko, A.E., Zhuravlyov, V.A., Semyonova, L.R., Tokarev, M.Y., 2018. Development history and quaternary deposits of the White Sea basin. In: Lisitsyn, A., Demina, L. (Eds.), Sedimentation Processes in the White Sea. The Handbook of Environmental Chemistry, vol. 82. Springer, Cham.
- Saarnisto, M., 1970. The late weichselian and flandrian history of the Saimaa lake. Comment. Phys. Math. 37, 107.
- Saarnisto, M., 2012. Late Holocene land uplift/neotectonics on the island of valamo (Valaam), Lake Ladoga, NW Russia. Quat. Int. 260, 143–152.
- Saarnisto, M., Grönlund, T., Ekman, I., 1995. Lateglacial of lake Onega – contribution to the history of the eastern Baltic basin. Quat. Int. 27, 111–120.
- Saarnisto, M., Grönlund, T., 1996. Shoreline displacement of lake Ladoga – new data from kilpolansaari. Hydrobiologia 322, 205–215.
- Saarnisto, M., Saarinen, T., 2001. Deglaciation chronology of the scandinavian ice sheet from the lake Onega basin to the Salpausselkä end moraines. Global Planet. Change 31, 387–405.
- Saltykova, V.F., Travina, M.A., 1977. Stratigraphy of Middle and Late Pleistocene sediments of northeastern Ladoga region based on pollen and diatom data. In: Salomon, A.P. (Ed.), Proceeding of Ministry of Geology of RSFR, vol. 6. Geological fund of RSFR, Moscow, pp. 92–99 (in Russian).
- Sauramo, M., 1958. Die geschichte der Ostsee. *Annales Academiae Scientiarum Fennicae*, Series A 3 (51), 522.
- Saveljeva, L.A., Andreev, A.A., Gromig, R., Subetto, D.A., Fedorov, G.B., Wennrich, V., Wagner, B., Melles, M., 2019. Vegetation and climate changes in northwestern Russia during the Lateglacial and Holocene inferred from the Lake Ladoga pollen record. Boreas 48, 349–360.
- Sharp, R.P., 1949. Studies of superglacial debris on valley glaciers. Am. J. Sci. 247, 289–315.
- Sissons, J.B., 1980. Paleo-climatic inferences from loch lomond advance glaciers. In: Lowe, J.J., Gray, J.M., Robinson, J.E. (Eds.), Studies in the Late Glacial of North West Europe. Pergamon Press, Oxford, pp. 31–43.
- Sorokin, A.I., Naumenko, M.A., Veselova, M.F., 1996. New morphometrical data of lake Ladoga. Hydrobiologia 322, 65–67.
- Stroeven, A.P., Heyman, J., Fabel, D., Björck, S., Caffee, M.W., Fredin, O., Harbor, J.M., 2015. A new Scandinavian reference  $^{10}\text{Be}$  production rate. Quat. Geochronol. 29, 104–115.
- Stroeven, A.P., Hättestrånd, C., Kleman, J., Heyman, J., Fabel, D., Fredin, O., Goodfellow, B.W., Harbor, J.M., Jansen, J.D., Olsen, L., Caffee, M.W., Fink, D., Lundqvist, J., Rosqvist, G.C., Strömberg, B., Jansson, K.N., 2016. Deglaciation of fennoscandia. Quat. Sci. Rev. 147, 91–121.
- Subetto, D.A., 2009. Lake Sediments: Paleolimnological Reconstructions. Herzen State Pedagogical University, St. Petersburg, p. 343 (in Russian).
- Subetto, A.D., Davydova, N.N., Ryalko, A.E., 1998. Contribution to the lithostratigraphy and history of lake Ladoga. Palaeogeogr. Palaeoclimatol. Palaeoecol. 140, 113–119.
- Svendsen, J.I., Alexanderson, H., Astakhov, V.I., Demidov, I., Dowdeswell, J.A., Funder, S., Gataullin, V., Henriksen, M., Hjort, C., Houmark-Nielsen, M., Hubberten, H.W., Ingólfsson, Ó., Jakobsson, M., Kjær, K.H., Larsen, E., Lokrantz, H., Lunkka, J.P., Lyså, A., Mangerud, J., Matiouchkov, A., Murray, A., Möller, P., Niessen, F., Nikolskaya, O., Polyak, L., Saarnisto, M., Siegert, C., Siegert, M.J., Spielhagen, R.F., Stein, R., 2004. Late Quaternary ice sheet history of northern Eurasia. Quat. Sci. Rev. 23, 1229–1271.
- Waldmann, N., Ariztegui, D., Anselmetti, F.S., Coronato, A., Austin Jr., J.A., 2010. Geophysical evidence of multiple glacier advances in Lago Fagnano ( $54^{\circ}\text{S}$ ), southernmost Patagonia. Quat. Sci. Rev. 29, 1188–1200.
- Zaremba, N.J., Scholz, C.A., 2019. High-resolution seismic stratigraphy of late pleistocene glacial Lake iroquois and its Holocene successor: Oneida Lake, New York. Palaeogeogr. Palaeoclimatol. Palaeoecol. 534, 109286.